Dissertation

Theoretical Studies on Dissociation Process of Plastocyanins Complex by using Parallel Cascade Selection Molecular Dynamics Simulations

Graduate School of

Natural Science & Technology

Kanazawa University

Divison of Mathematical and Physical Science

Student ID No.: 1824012007

Name: Dian Fitrasari

Chief Advisor: Prof. Hidemi Nagao

Date of Submission: April 21st, 2022

Contents

List of Figures

List of Tables

Acknowledgement

First of all, I want to express my gratitude to Allah Subhanahu Wata'ala for His loving and caring which makes me can go far until this point.

I would like to express my sincere gratitude for my supervisor Prof. Hidemi Nagao which all his patience, knowledge for guiding me go far with this doctoral journey. His supervision during my doctoral journey help me a lot in all time which I passed during this Ph.D program. I would like to express my sincere gratitude also for Prof. Kazutomo Kawaguchi with the valuable discussion, suggestion and help during my Ph.D journey. I also want express my sincere gratitude to Prof. Mineo Saito, Prof. Fumiyuki Ishii, Prof. Tatsuki Oda and Prof. Hiroshi Iwasaki during my Ph.D program, without their help and suggesstion I will not pass this journey until this day.

All my deepest sincere gratitude to all the member of Computational Science Laboratory: Kak Arwan, Kataoka-san, Saito-san, Maeda-san, Shibata-san, Nakagawa-san, Takagi-san, Matsura-san, Habibi, Mutiara, Helmia, Kodama-san, Teh Lilih, Stephanie, Beryl, Venia.

My sincere gratitude for all the doctors, nurse, all of the employment of Morinosato Clinic, Kanazawa Medical Center and Kanazawa University Hospital. I will not go far during my Ph.D journey without their help. All my deepest sincere gratitude for Indonesia's Students and Community, Aflah, Teh Muti, Mba Hikmah, Bu Monika, Hana, all Double Degree Program (DDP) students, Maya. Thank you for the help and caring during my time in Kanazawa.

My sincere gratitude to Kanazawa University which gave me this opportunity to enroll in Kanazawa University with this DDP program, also for the financial support which gave to me during this program. I also want to delivered my sincere gratitude to Institut Teknologi Bandung (ITB) to give me this opportunity, especially for my supervisor Prof. Dr. Suprijadi, M.Eng. and Acep Purqon, Ph.D.

Last but not least, for my family which always there and never giving up to believe.

For all people which help me during this journey which maybe I can not write it all. Thank you, thanks for all the kindness and care that showed to me during this time. Hope the almighty give all the kindness for you all.

Abstract

The sytem in photosystem I is one of the important photochemical machines which convert light into chemical energy in photosynthesis which produce oxygen. The membrane complex contains 10 until 30 protein subunit that harvest the light and electron transfer. Photosystem I operates efficiency in quantum level and sets energy ceiling [1].

One of large multisubunit complex in electrons transfer from PSII to PSI is cytochrome b6f complex. The mobile electron carrier is Plastocyanin with molecular weight 10-kDa Cu. The location of this electron carrier in the lumen of the choloroplast thylakoid. Plastocyanins shuttles electron from cytochrome f in the cytochrome b6f complex to P700 in PSI. Its replaced by cytochrome (cytochrome c6) in green algae and cyanobacteria under deficiency copper [2].

In this research, we have been presenting procedure to calculate the complex Plastocyanin. We use two kinds of model, all-atom model and MARTINI coarse-grained method. We searching for association-dissociation pathways using Parallel Cascade Selection Molecular Dynamics (PaCS-MD). We analyze free energy landscape (FEL) using multiple independent umbrella sampling (MIUS) with weighted histogram analysis (WHAM) method.

We find that binding free energy using all-atom model is around 3 kcal/mol and that the barrier energy at around the middle range between the equilibrium point and the dissociation state becomes about 1 kcal/mol from the association process. The present results suggest that the energy barrier may arise from hydrogen bonds between two plastocyanins. We also find that the effective interaction between two plastocyanins already vanishes at the distance of $2\mathring{A}$ from equilibrium state. The equilibrium point of the complex around 27.9 $\mathring{A}$ is a good agreement with the experimental result 27.8 $\mathring{A}$.

We find the free energy binding using MARTINI coarse-grained for complex Plastocyanin is around 20 kcal/mol. We find the barrier in COM distance between the middle range of equilibrium point. This results suggest that the barriers which we find through the FEL may be arise because the protonation from histidine. We also found that the effective interaction vanish 4 from equilibrium state. The equilibrium point is around $23\mathring{A}$.

1 Introduction

1.1 Photosynthetic System and Plastocyanins

The photosynthetic system has a complex mechanism. The photosynthetic transport chain includes electron transfer in its mechanism. This mechanism happens in higher plants, algae, and cyanobacteria [2]. In a photosynthetic system as known, many chemical reactions are happening. This reaction changes the inorganic material to organic material. The inorganic material contains carbon dioxide CO_2 and water H_2O. The organic material is carbohydrate $C_6H_12O_6$ and oxygen O_2. This reaction happens in leaves chlorophyll, specifically in the thylakoid membrane. In the thylakoid membrane, there is some disk shape part called a granum. In this place, some chemical anoxygenic reactions happen to convert energy. This chemical reaction becomes some cycle that makes electron transfer from one part in the thylakoid membrane into another part.

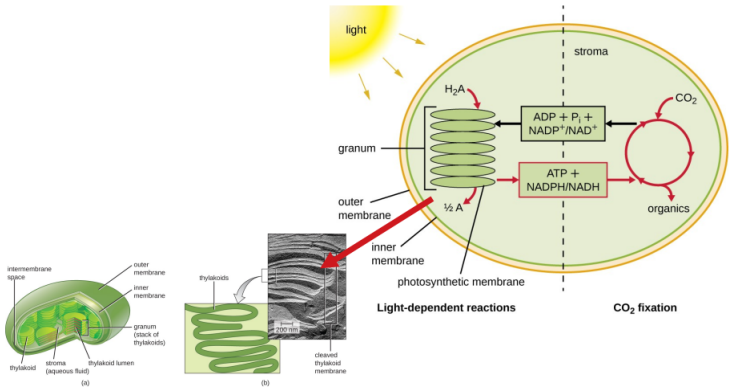

Figure 1.1: The Photosynthetic System.

One chemical reaction in this process is called photosystems I and II. In this photosystem process, some proteins interact with one another to transfer electrons. The first photosystem which is happening is photosystem II, in grana for cyanobacteria, and other higher plants.

In the photosynthetic system, there are two light reactions. It is divided into the mechanism in photosystem I and photosystem II. This process produces molecular oxygen, reduces nicotinamide

adenine dinucleotide phosphate to nicotinamide adenine dinucleotide phosphate-oxidase, and synthesizes adenosine triphosphate.

The system in photosystem one is one of the important photochemical machines which convert light into chemical energy in photosynthesis which produces oxygen. The membrane complex contains 10 until 30 protein subunits that harvest the light and electron transfer. Photosystem I operates efficiency in quantum level and sets energy ceiling [1].

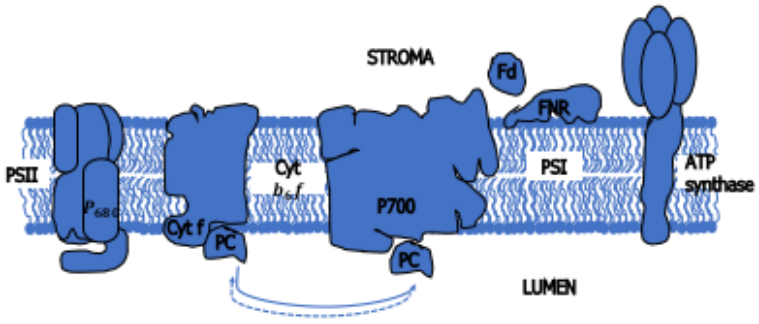

Figure 1.2: The Photosystem I and II.

One of the large multisubunit complexes in electrons transfer from PSII to PSI is the cytochrome b6f complex. The mobile electron carrier is Plastocyanin with a molecular weight of 10-kDa Cu. The location of this electron carrier in the lumen of the chloroplast thylakoid. Plastocyanins shuttles electrons from cytochrome f in the cytochrome b6f complex to P700 in PSI. Its replaced by cytochrome (cytochrome c6) in green algae and cyanobacteria under deficiency copper [2].

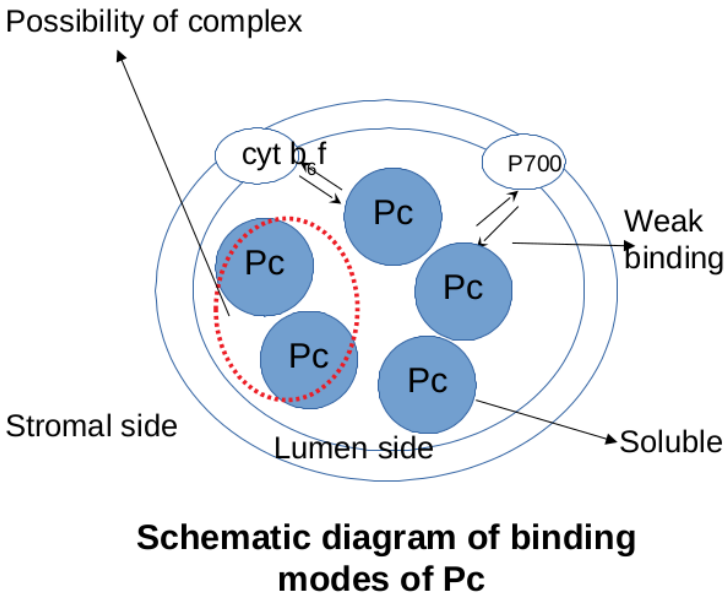

Figure 1.3: The Schematic Diagram of Binding Modes of Plastocyanin.

Plastocyanins have a unique characteristic that makes them known as one kind of blue protein. Its because in the active site, Plastocyanins have copper (Cu) which makes them different from other proteins. The structure of Plastocyanins at the atomic level describes as hydrophobic residues which have β-barrel in their interior. The site-directed mutagenesis of Pc proves to be useful from the structure-function relationship.

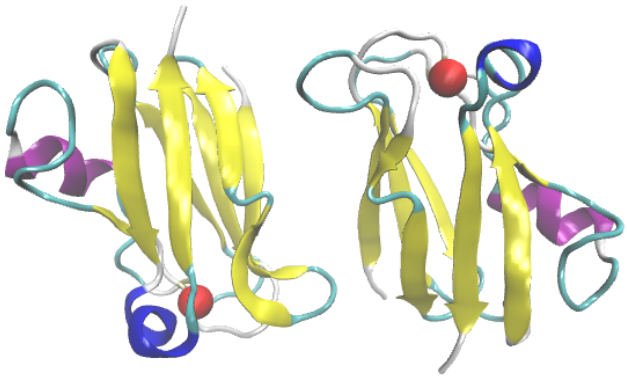

Figure 1.4: Plastocyanins from *A. variabilis* PDB ID: 2GIM [3].

Mainly two spectroscopic techniques, optical and EPR spectroscopy, have been used to investigate how the copper-site is affected by different mutations. The redox properties of the mutants have been investigated and factors that affect the reduction potential are discussed. Absorption and EPR spectra and reduction potentials for the surface mutants are similar to those of the corresponding wild-type. However, mutants around the Cu ion affected the mentioned properties. Comparisons are made with other ferredoxins. Five site-directed mutants of spinach Pc, Pc(Leu12His), Pc(Leu15His), Pc(Thr79His), Pc(Lys81His), and Pc(Tyr83His), have been modified by covalent attachment of photoactive ruthenium (Ru)-complex at the surface-exposed histidine residues. The rates of the internal electron-transfer reactions exhibit an exponential dependence on the metal-to-metal separation with a decay factor of 1.1 A-1. Reorganization energy for the Cu-to-Ru electron-transfer reaction of 1.2 eV was determined. Interprotein electron-transfer reactions involving genetically modified Pc are described. Ionic-strength and pH dependencies indicated that electrostatic interactions are involved in the complex formation between Pc and PS 1, which was confirmed by mutations in the acidic patches of Pc. A very specific interaction was further verified by replacements of hydrophobic residues. Position 10, 12, 36, 87, and 90 were found to be very important for the formation of an active complex. A comparison between available structures of Pc and cyt c6, both effective donors to PS 1, is made. The physiological electron donor to Pc, cyt f, is briefly described. [4]

1.2 Molecular Dynamics (MD)

Molecular dynamic simulation was developed in 1970 simulate biological systems which has several hundred of atoms, its include protein hydration with explicit solvent. The simulation of high performance computing (HPC) which have 50,000-100,000 atoms are commonly available. The molecular dynamic (MD) algorithm with HPC make significance improvement to calculate this large system. The experimental structure or modeling data has been used for initial model. There is the detail differences because the level of the details. Atomistic detail use for represent actual systems and coarse-grained for represent large system or long simulation. The real solvent which will describe the solvent effect in simulation, represent by the explicit solvent. The force-field

which has been deduce from molecular structure is obtained by forces acting once the system has build. The calculation for the force-field is easy but the equation is complex. The springs for bond length and angles, periodic functions for bond rotations and Lennard–Jones potentials, and the Coulomb's law for van der Waals and electrostatic interactions, has been representing in force-field representation which is make this representation for molecular feature much more simple. The parameter for force-fields in atomistic simulation was differ. Its not necessary interchangeable and not-all allowed for representing all type of molecule. However, the simulation by modern force-field are equivalent. The process for calculation, start from obtaining the force acting of individual atom, Newton's law of motion use for calculating acceleration and velocity for updating position of atom. The algorithm which is described the molecular dynamics simulation, shown by the figure below 5.

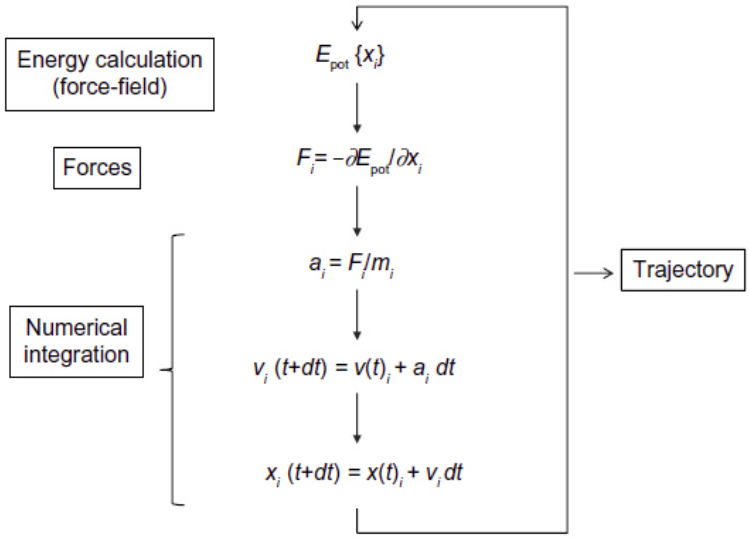

Figure 1.5: The algorithm of molecular dynamics simulation.

The instability which want to avoid can be done with makes the time step shorter than the fastest movements in molecule. Its ranks between 1-2 fs. The biological process has microsecond-long simulation. Its require the iteration of this calculation 109 times. The coarse-grained simulation has this strength. Its make representation simple, larger time step possible, and the simulation effective length extend. The accuracy expense of the simulation ensemble has obtain by this model.

The performance of MD simulation also improve by the advances of algorithm, fine-tuning of energy calculation, parallelization, or the use of graphical processing units (GPUs).

The process speeding up by the present generation of computers which takes benefit of parallelism and accelerators. The messaging passing interface (MPI) has compatible with simulation codes (AMBER, CHARMM, GROMACS, or NAMD). The MPI can reduce the computation time when the computer cores large number done simultaneously. The distribution among processors has used as general strategy for benefiting the interactions locally. In each processor, only a small fragment was simulated. The position in space represent the most efficient division. The particles whom represent there has irrespective space which the region of processor deals. The regions of simulating neighboring as the only one who share the information. The communication between processor is reduce. In simulation codes, the use of accelerator, mostly GPU, as mention before, become the major breakthrough. Once GPU has been used for handling the graphics of computer, and until now, can be applicable in atomistic MD simulation. The combination of GPU with MPI, become the default strategy of MD simulation [6].

As we mention before, there are several simulation codes such as AMBER, CHARMM, GROMACS, or NAMD. In this research for all-atom models we spesifically use CHARMM force field with NAMD package. One kind of general and flexible molecular simulation and model is CHARMM. It is use classical (empirical and semiempirical) also quantum mechanical (semiempirical or ab initio) energy functions for molecular systems of many different system.

As we mention before, there are several simulation code. One of them is CHARMM. In CHARMM the atom interaction, shown by the figure below.

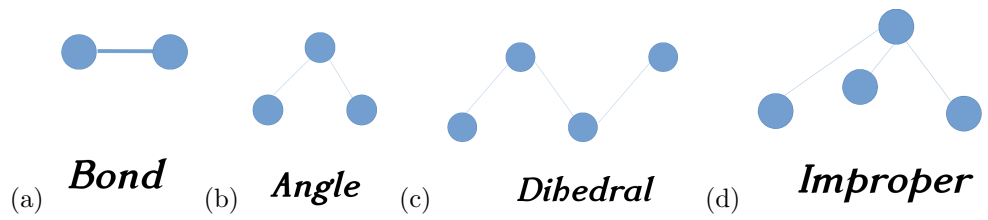

Figure 1.6: Bond interaction in CHARMM force field [7]. (a)Bond. (b) Angle. (c) Dihedral. (d) Improper.

The equation describe by the bonded interaction and non-bonded interaction which has shown in equation below.

$$V = \sum_{bonds} k_b \left(b - b_0\right)^2 + \sum_{angles} k_\theta \left(\theta - \theta_0\right)^2 + \sum_{dihedrals} k_\phi \left[1 + cos(n\phi - \delta)\right]^2 + \sum_{impropers} k_\omega \left(\omega - \omega_0\right)^2$$

$$+\sum_{Urey-Bradley} k_u \left(u - u_0\right)^2 + \sum_{nonbonded} \epsilon \left[\left(\frac{R_{min_{ij}}}{r_{ij}}^{12} - \frac{R_{min_{ij}}}{r_{ij}}^{6}\right)\right] + \frac{q_i q_j}{\epsilon r_{ij}} (1)$$

2 Purposes

The purposes of this research is to investigated the dynamics and interactions of two Plastocyanins by dissociation process with Parallel Cascade Selection Molecular Dynamic (PaCS-MD) Simulation, i.e.

1. To investigate the dissociation pathways two Plastocyanins using all-atom method with PaCS-MD simulation.
2. To investigate the dynamic of two Plastocyanins by root mean square deviation (RMSD) analysis .
3. To analyze the interaction between two Plastocyanins in dissociation process.
4. To investigated the free energy landscape of two Plastocyanins with Multiple Independent Umbrella Sampling (MIUS) and Weighted Histogram Analysis (WHAM) methods.

3 Methodology

3.1 Parallel Cascade Selection Molecular Dynamic (PaCS-MD)

PaCS-MD is proposed as a molecular simulation method to generate conformational transition pathway under the condition that a set of “reactant” and “product” structures is known a priori.

In PaCS-MD, the cycle of short multiple independent molecular dynamics simulations and selection of the structures close to the product structure for the next cycle are repeated until the simulated structures move sufficiently close to the product [8] shown in Figure 1.1.

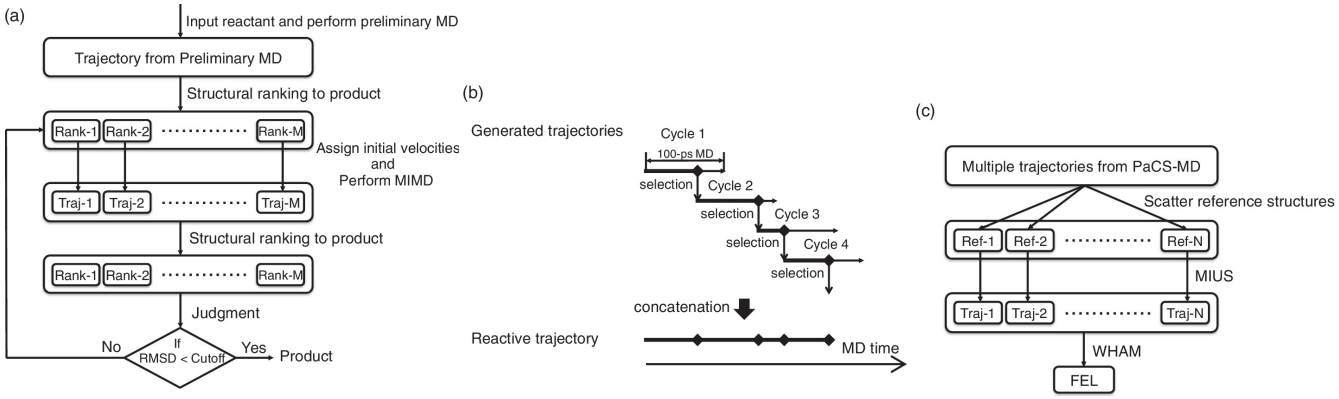

Figure 3.1: The flowcharts of Parallel Cascade Selection Molecular Dynamics (PaCS-MD) and analysis [8]. (a)Algorithm of PaCS-MD. (b) The selection of the cycle. (c) Free Energy Landscape (FEL) Analysis.

In this research, we try to modified the judgement for rank the ten structure. We use the center of mass distance between (COM) two proteins instead the root mean square deviation (RMSD) value. We try to divide it, into two pathways. The structure with COM lower than the experimental value, will be choose in reactive trajectories for association pathways. The structure with COM bigger than the experimental value, choose as the dissociation pathways. The scheme which explain how we choose the reactive trajectories, shown in picture below,

Figure 3.2: The differences between PaCS-MD algorithm by Harada et. al. [8] and with this research (right side with blue box).

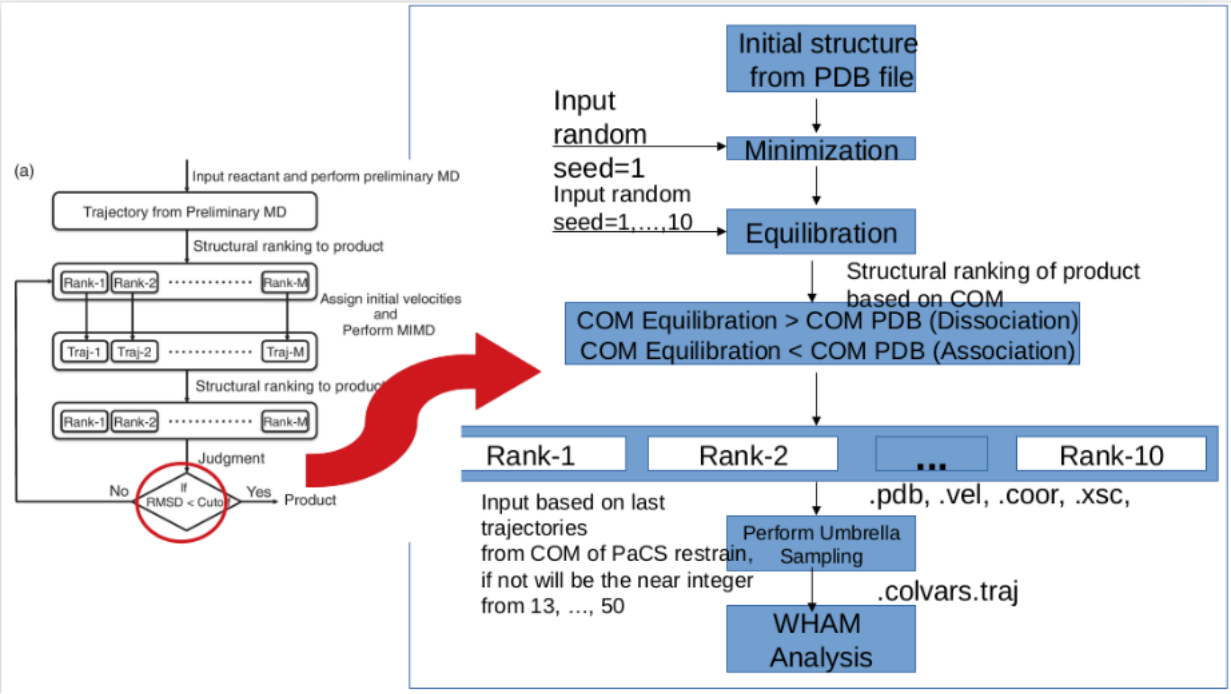

4 Introduction of Calculation Analysis

4.1 Center of Mass between the distance of protein complex

The distance {...} block defines a distance component between the two atom groups, group1 and group2 [**?**]. The center of mass function is slightly harder because you have to get the mass as well as the x, y, z values, then break that up into to components. The formula for the center of mass as [9] follows:

$$\frac{\sum m_i x_i}{\sum mass_i} \tag{2}$$

4.2 Root Mean Square Deviation (RMSD) [10]

The block rmsd $\{...\}$ defines the root mean square replacement (RMSD) of a group of atoms with respect to a reference structure. For each set of coordinates $x_1(t), x_2(t), ..., x_N(t)$, the colvar component rmsd calculates the optimal rotation $U^{\left\{x_i(t)\to x_i^{(ref)}(t)\right\}}$ that best superimposes the coordinates $x_i(t)$ onto a set of reference coordinates $x_i^{(ref)}(t)$. Both the current and the reference coordinates are centered on their centers of geometry, $x_{cog}(t)$ and $x_{cog}^{(ref)}$. The root mean square displacement is then defined as:

$$RMSD(\{x_i(t)\}, x_i^{(ref)}) = \sqrt{\frac{1}{N}\sum_{i=1}^{N} |U(x_i(t) - x_{cog}(t)) - (x_i^{(ref)} - x_{cog}^{(ref)})|^2}, \tag{3}$$

The optimal rotation $U^{\left\{x_i(t)\to x_i^{(ref)}(t)\right\}}$ is calculated within the formalism developed in reference [**?**], which guarantees a continuous dependence of $U^{\left\{x_i(t)\to x_i^{(ref)}(t)\right\}}$ with respect to $\{x_i(t)\}$

4.3 Free energy landscape (FEL) calculation with multiple independent umbrella sampling (MIUS)

In MIUS, a set of umbrella potentials ($V^i_{umbrella}$) (i = 1, 2, ..., N),

$$F = V^i_{umbrella} = k_i(\overrightarrow{r}^{CoM} - \overrightarrow{r}^{CoM_0})^2, \tag{4}$$

is applied to the distance between center of mass position of Pc/Pc, where N is the total number of MIUS and ki (i = 1, 2, ..., N) are the force constant for positional restraints. Here, the reference and initial structures are selected from the reactive trajectories.

4.4 Weighted Histogram Method

The optimal probability density ρ_0 is calculated as a linear combination of the reweighted probability densities ($\rho^{unbiased}$) (i = 1, 2, ..., N) from MIUS with the weighted histogram analysis method (WHAM),

$$\rho_0 = C \sum_{i=1}^{N} \omega_i \rho_1^{unbiased} \begin{cases} \frac{\partial \sigma^2[\rho]}{\partial \omega_i} = 0 \\ \sum_{i=1}^{N} \omega_i = 1 \end{cases} \tag{5}$$

where C is a normalization constant. The set of (w_i) (i = 1, 2, ..., N) is weighting factors to be determined so as to minimize a statistical error σ^2 $[\rho_0(\xi)]$ under the normalization condition in Equation. Finally, free energy F is calculated as the logarithm of the optimal probability density:

$$F = -k_B T \, ln\rho_0 \tag{6}$$

where k_B and T are Boltzmann constant and temperature [**?**].

5 Calculation Condition

Plastocyanin from X-ray diffraction which is solved by Schmidt, et al. (PDB ID: 2GIM) [3] is used as the initial structure for the simulation of dissociation process. Plastocyanin consists of 105 amino acid residues, and two copper ions in its active site. We perform Parallel Cascade Molecular Dynamics (PaCS-MD) for two kind of models which is all-atom model and MARTINI coarse-grained model. The premelinary MD is used to generate initial structure for PaCS-MD. This initial structure, then divide in to ten independent simulation as known as short Multiple Independent Molecular Dynamics (MIMD) simulation [8]. The ten independent simulation differentiate

by the number of seed (random seed) from 1 to 10. The center of mass distance between two plastocyanin use as the ranking measure. The furthest distance choose as reactive trajectories for dissociation pathways. This reference structure will be use as initial structure in free energy landscape (FEL) analysis. Multiple independent umbrella sampling (MIUS) with weighted histogram analysis method (WHAM) is used to analyze the free energy landcape [8].

In this calculation, we use NAMD2.12 software program package[11]. The force field parameters used are CHARMM22[7],[12] and TIP3P water model [13]. The timestep that we perform during this simulation is 2fs/step. For all atom model, the box size is 70 $\mathring{A}$×59 $\mathring{A}$×100 $\mathring{A}$. NPT ensemble is applied to this simulation at 310 K and 1 atm. The cutoff distance is 12 $\mathring{A}$. NPT ensemble is applied to this simulation with 310 K and 1 atm.

6 Result and Discussion

All-atom molecular dynamic simulations of two plastocyanins are performed by using the initial configuration of the crystal structure with PDB ID 2GIM[3]. The detail of parameters for MD simulation is provided in Table 8.1.

Table 6.1: The parameters of All-Atom-MD Simulation.

Parameters	Identities (AA-MD Simulation)	Identities (PaCS-MD Simulation)
Simulation Program	NAMD 2.12 for linux 64-bit Intel/AMD single node	NAMD 2.12 for linux 64-bit Intel/AMD single node
Force Field	CHARMM22	CHARMM22
Time Step	2fs/step	2fs/step
Solvent	TIP3 model	TIP3 model
Box size	55.739 Å x 44.899 Å x 78.494 Å	55.739 Å x 44.899 Å x 78.494 Å
The number of water	13032	31229
Counter Ion	2 Na^+, 2 Cl^-	2 Na^+, 2 Cl^-
Temperature Control	Langevin Thermostat	Langevin Thermostat
Pressure Control	Langevin Piston	Langevin Piston
Ensemble	NPT	NPT
Cutoffs	12 Å	12 Å
Number of M runs	-	10 structure each MIMD
Simulation time	-	5 ns each MIMD

In table above, we can see that there are two kinds of parameters that we use. In order to differentiate the system that using all-atom MD and all atom PaCS-MD. The parameters which set to be different is the number of M runs. The number of M runs differentiate by using the number of seed. The number of seed that selected has number from one to ten. The number of seed have function to determined the exact position and velocity.

The equilibrium state of the complex system which is obtained from reactive trajectories PaCS-MD All-atom molecular dynamic shown in Figure 6.1 shows the dependence of distance between center of mass of two plastocyanins coloured in red and of distance between two copper ions in blue dashed line. From Figure 6.1 the average of two center of mass becomes around 31 $\mathring{A}$ for 1.7ns time simulation. In this analysis, we can see that the two Plastocyanins makes repulsive interaction from one and another. It shown with the value of COM which has been bigger than experimental value.

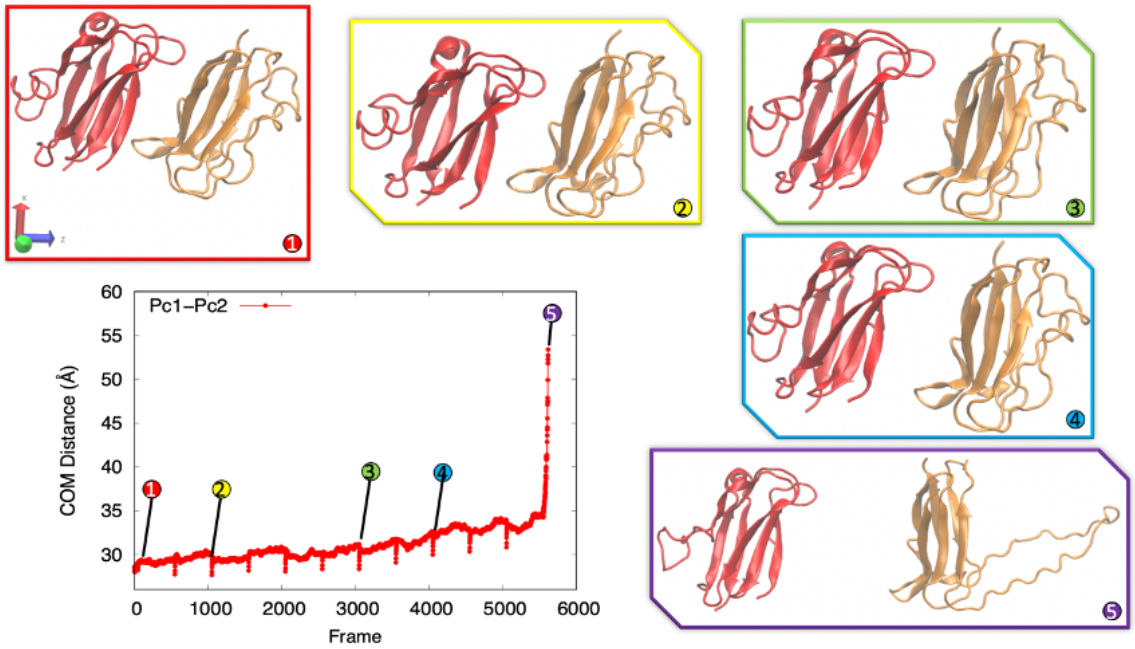

Figure 6.1: The red line represent the distance between center of mass of two Plastocyanin corresponding to PDB file (PDB ID:2GIM) from PaCS-All-Atom-MD for describing the dissociation pathway of two complex plastocyanin. Reactive trajectories are obtained by PaCS All Atom-MD simulations (5.6ns).

In Figure 6.1. the red solid, blue dashed and yellow dotted lines correspond to RMSD of the one plastocyanin, another plastocyanin, and the complex system, respectively. We can see the value which has stable, but has been increase significantly in last frame. In this case, we decide to avoid the structure and using the reactive trajectories from one until four in Figure 6.1. We assume this happen may be because the reactive trajectories for this state happen in another number of seed.

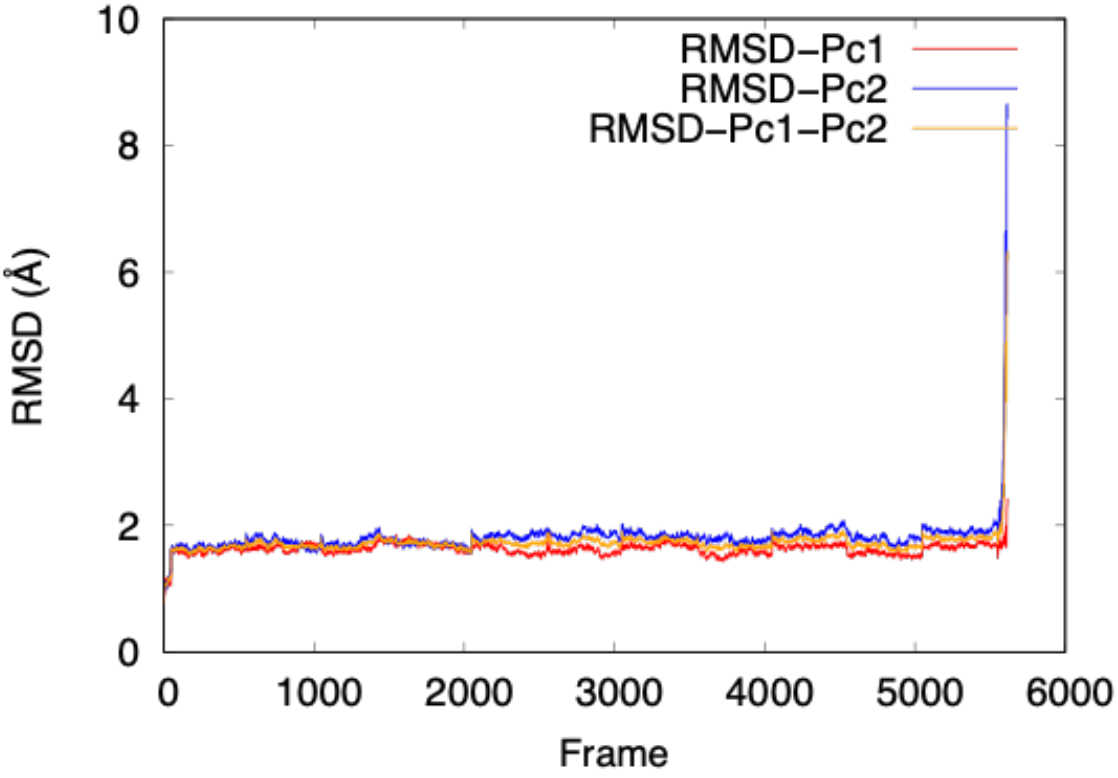

Figure 6.2: RMSD shown as time function that represent with frame, each frame steps correspond to 10 ps.

The equilibrium state of the complex system is obtained shown in Figure 6.3. In this Figure 6.3 first row, the red solid line corresponds to RMSD of chain A in complex plastocyanin. The blue dashed line corresponds to RMSD of chain C. The yellow dashed line corresponds to all chain in complex plastocyanin. In Figure 6.3 second row, the average distance of two centers of mass becomes around 34 $\mathring{A}$ for 70ns simulation time. Meanwhile in experimental data the average center of mass is 27.847 $\mathring{A}$. The red solid line corresponds to the center of mass distance (COM) between two plastocyanins and the yellow dashed line corresponds to the distance between two copper ions in complex plastocyanin. The difference between this calculation and experimental data shown in tabel below.

Structure	Distance (Å), Experimental data [3]	This calculation
(Pc1)-(Pc2)	27.847	27.9
(Pc1)Cu-Cu(Pc2)	33.169	35

Table 6.2: Center of Mass Distance 2 Plastocyanin (PDBID:2GIM).

Figure 6.3 shown the analysis differences of All-Atom MD in the left side and PaCS-MD in the right side. The first row show the RMSD analysis and second row for center of mass distance analysis. There are three state which describe the Plastocyanins dissociation. The first state is equilibrium state, the second is transition state and the third is dissociation state. The equilibrium state show the Plastocyanins condition after equilibration.

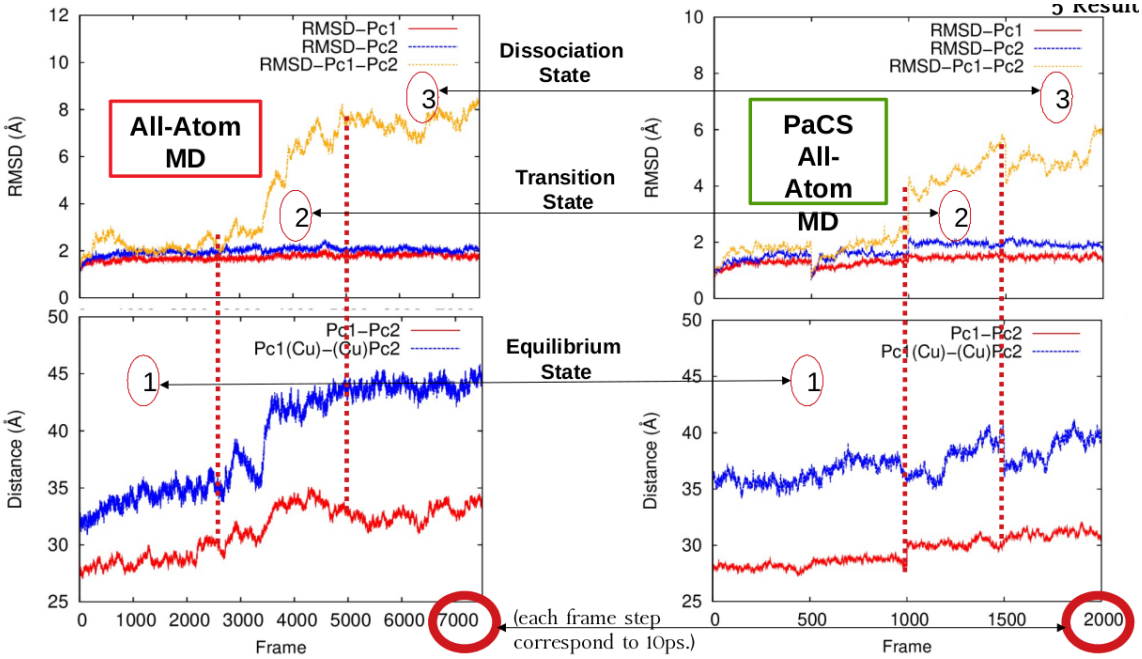

Figure 6.3: The analysis differences of All-Atom MD (left side) and PaCS-MD (right side). First row for RMSD analysis and second row for center of mass distance analysis.

From Figure 6.3 the equilibration value has a good agreement with experimental equilibrium point which is around 28 $\AA$. This condition show that Plastocyanin chain A still have close contact with Plastocyanin chain C. The conformational structure condition shown in Figure 6.4. In Figure 6.4 for Plastocyanins in All-Atom MD simulation. The amino acid which is contact in close distance shown in Figure 6.4. We can see that the surface of Plastocyanins bind to one and another.

Figure 6.4: The conformational structure of Plastocyanin (PDBID:2GIM) in equilibrium state All-Atom MD

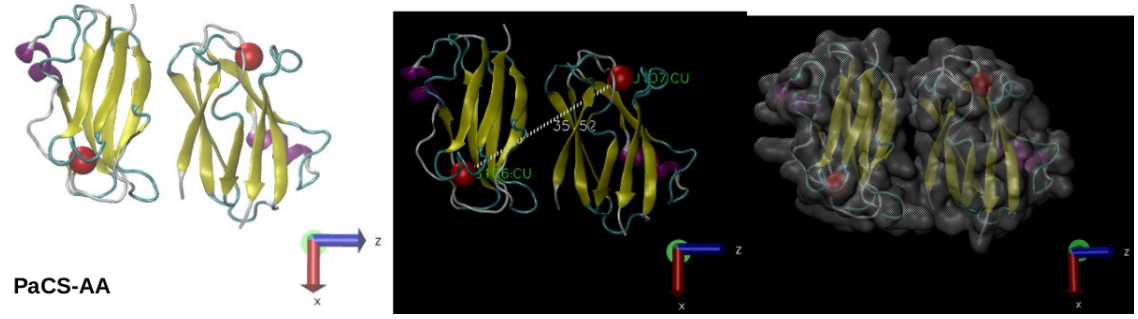

Figure 6.5: The conformational structure of Plastocyanin (PDBID:2GIM) in equilibrium state PaCS-MD

In Figure 6.5, the Plastocyanins entering the transition state. We can see that Plastocyanins start to dissociate but still not fully dissociating. We can find this transition state has high value of barriers energy which shown later in Figure 6.10. This high value relate to the movement of water from Plastocyanins surface that has close contact between one and another, which is shown in equilibrium state before.

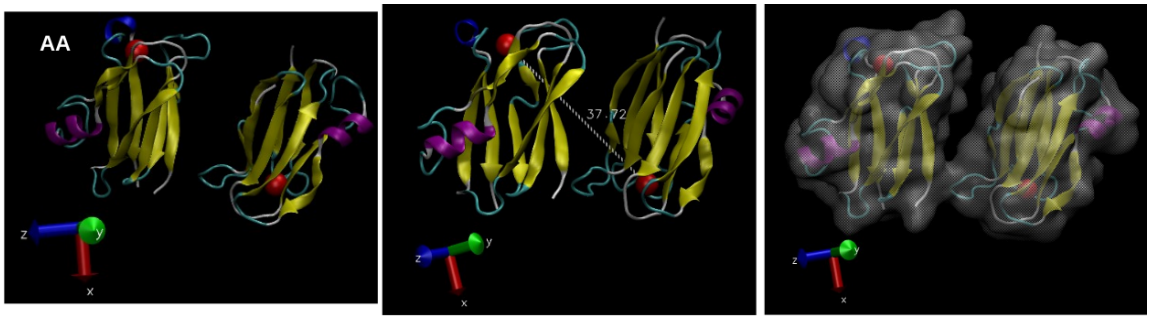

Figure 6.6: The conformational structure of Plastocyanin (PDBID:2GIM) in transition state All-Atom MDD

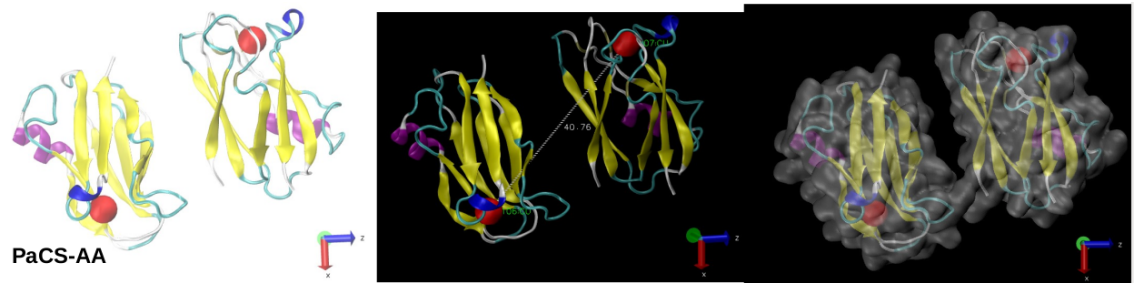

Figure 6.7: The conformational structure of Plastocyanin (PDBID:2GIM) in transition state PaCS-MD

In this Figure, we can see that the Plastocyanins has fully dissociate. In free energy landscape (FEL) analysis in figure 6.10 we can see that, in this state the energy value has converge which means the innteraction of Plastocyanins has been stable. We can confirm this stability also in RMSD value which has mention before.

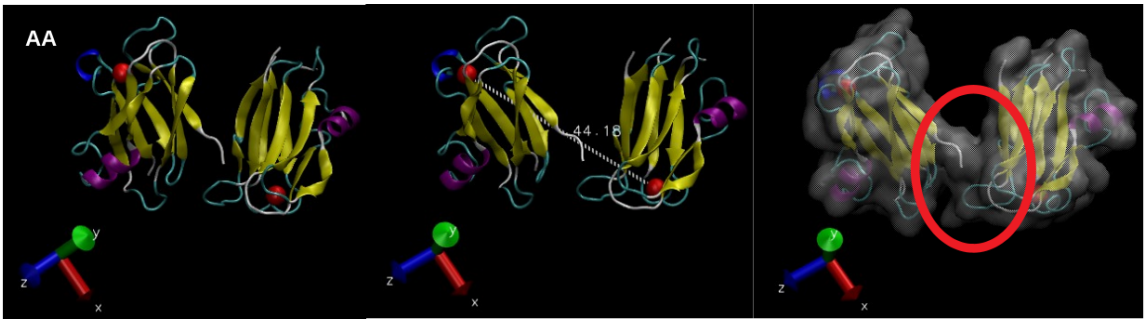

Figure 6.8: The conformational structure of Plastocyanin (PDBID:2GIM) in dissociation state All-Atom MD

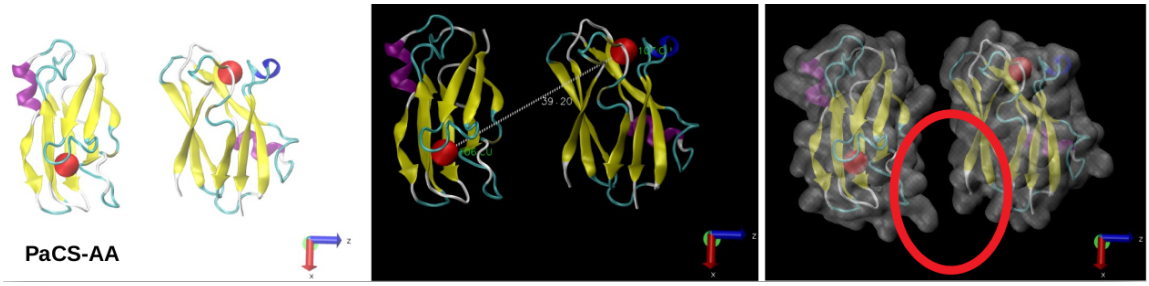

Figure 6.9: The conformational structure of Plastocyanin (PDBID:2GIM) in dissociation state PaCS-MD

Figure 6.10 shows a free energy landscape of dissociation process of the two plastocyanin proteins. We can find that the free energy landscape equilibrium point become 27.9 $\AA$ which has good agreement with the experimental equilibrium point. We can observe the free energy barrier around

29 $\mathring{A}$, which may arise from hydrogen bonds between two plastocyanins. The barrier energy for association process is around 1 kcal/mol. The binding free energy of two plastocyanins becomes around 3 kcal/mol. From the free energy landscape (FEL) shown in Figure 6.10, we observe the convergence of free energy around 30 $\mathring{A}$ to 32 $\mathring{A}$. We also suggest that the dissociation state of two plastocyanin can be found at those distance 31 $\mathring{A}$ which is shown in Figure 6.10. The short distance of dissociation state may be arising from the characteristic structure of plastocyanin which means the small and hard protein. In Figure 6 there are 8 β-sheet in yellow arrow and 1 α-helix in purple in one plastocyanin, and the gray strings correspond to the turn structure.

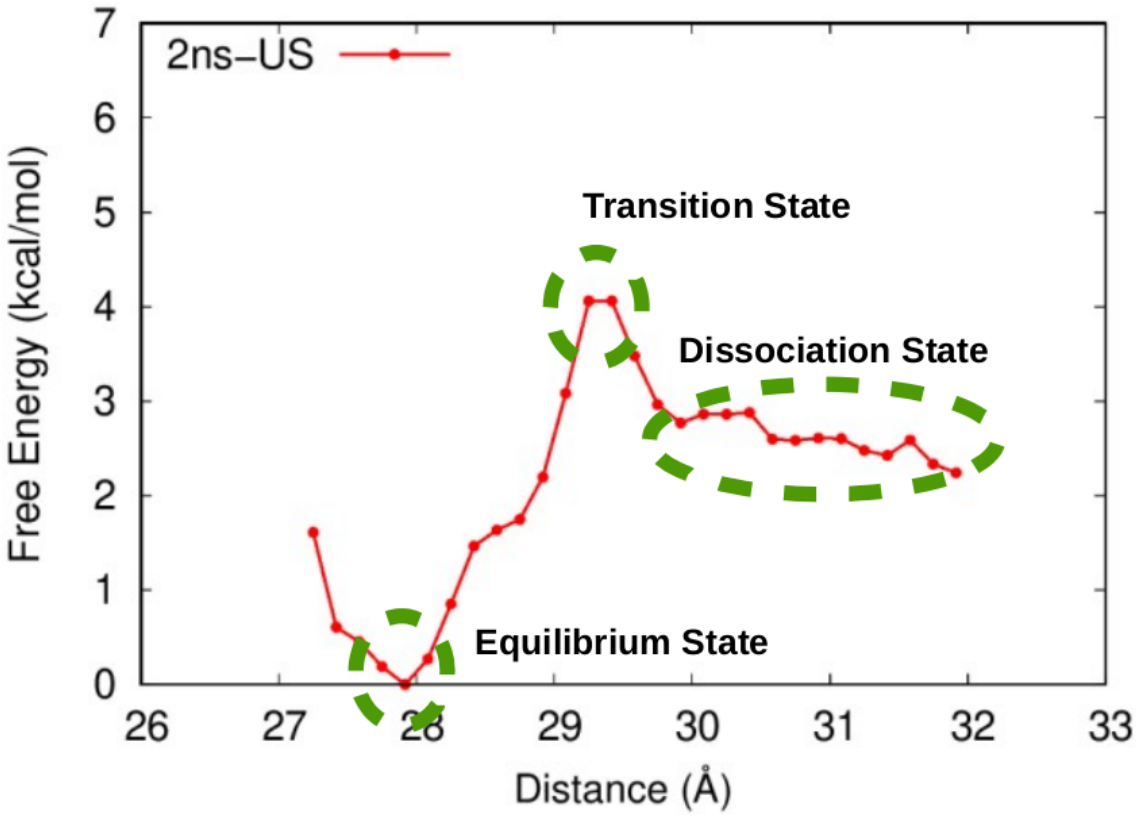

Figure 6.10: The free energy landscape analysis by PaCS-MD with MIUS and WHAM analysis.

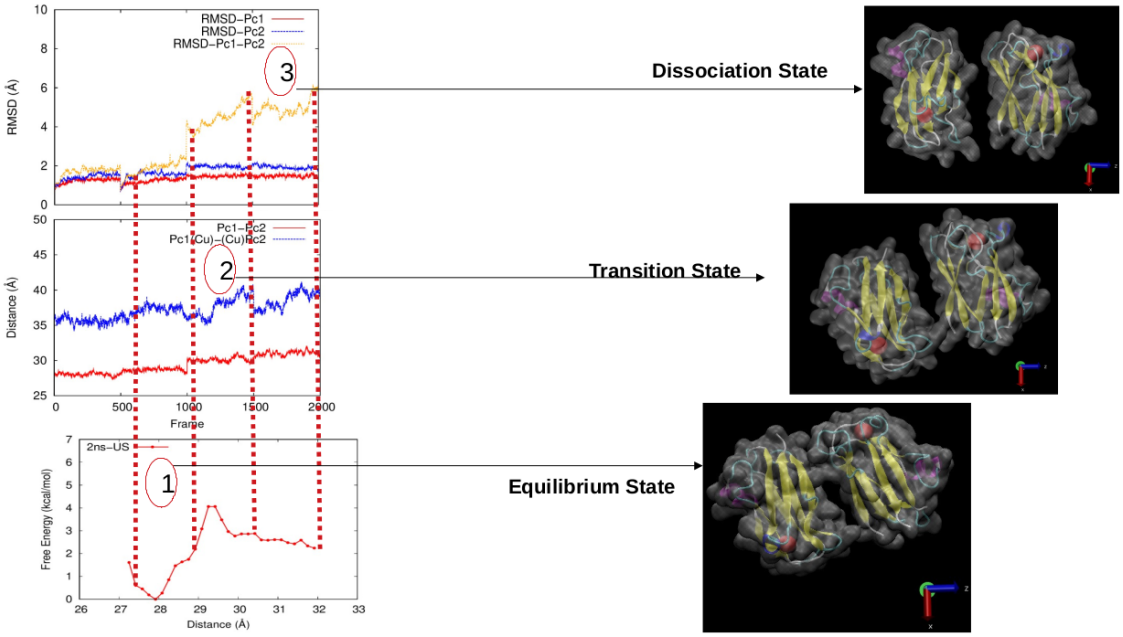

Figure 6.11: The free energy landscape analysis (comparison with RMSD and COM distance).

The analysis of solvent accessible surface area (SASA) shown in figure below. This analysis show how much the water molecule that has been contact with proteins in the surface. It also shown that differences of this value has a lot meaning to makes that each state has different value. It means some water molecule has been move from center of two Plastocyanins to another side. It makes the assumption that in equilibrium state which has close contact of Plastocyanins has the lowest value and the dissociation state has the biggest value of SASA analysis. This means there are some energy to move the water from another side to the center of two Plastocynins. The spesific analysis of this interaction will be shown in number of water analysis.

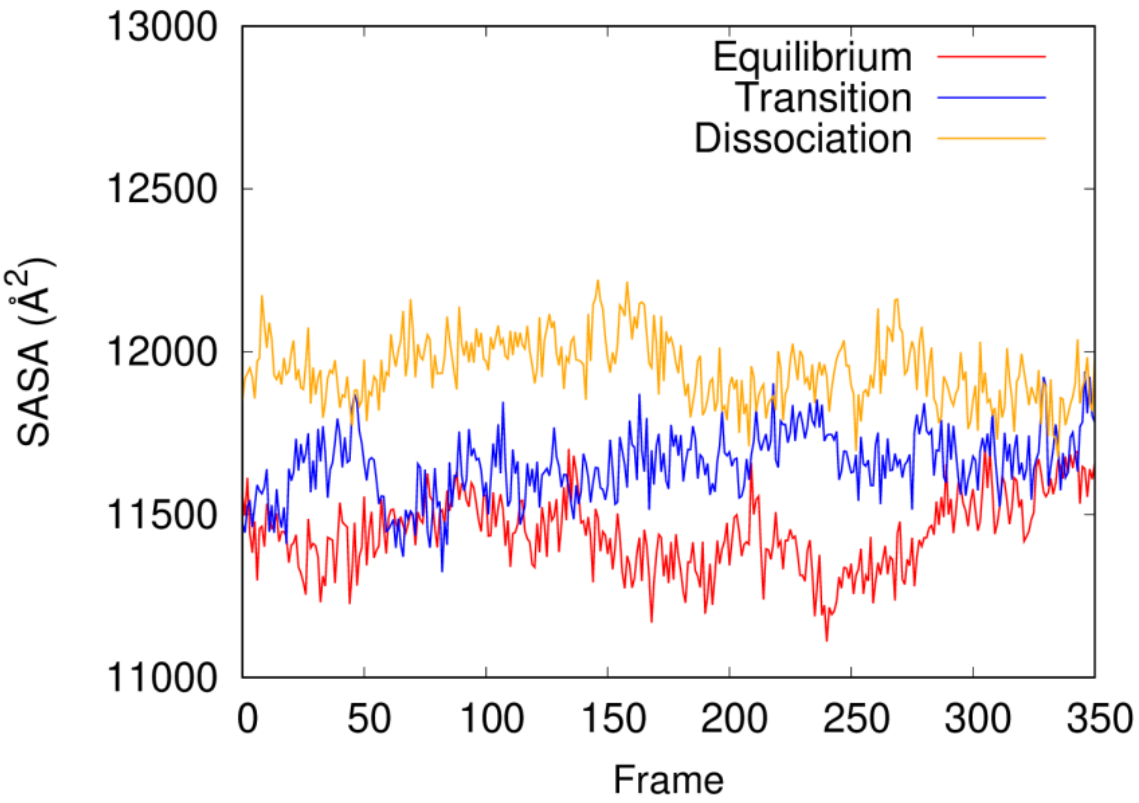

Figure 6.12: Solvent Accessible Surface Area (SASA).

Figure 6.13 shown the representation of the water molecule which is in equilibration state. We can see there are not so much water that interact in the center of Plastocyanins in this state. In Figure 6.14 we can see there are some water molecule that move in the center of Plastocyanins. In Figure 6.15 the water molecule which is move is much more than in the transition state. This representation make as can descrive there are some water molecule which move during the dissociation process of Plastocyanins. The water which has move shown in the value of barrier energy in Figure 6.17.

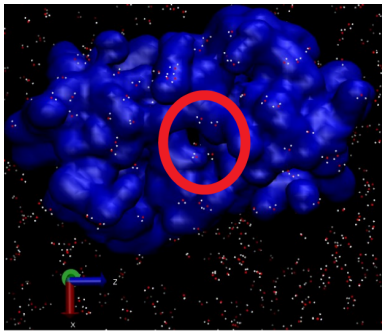

Figure 6.13: The conformational structure of Plastocyanin (PDBID:2GIM) with water contact representation Equilibrium State.

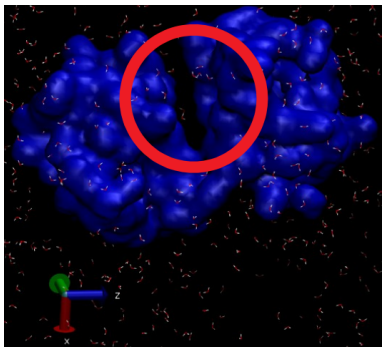

Figure 6.14: The conformational structure of Plastocyanin (PDBID:2GIM) with water contact representation Transition State.

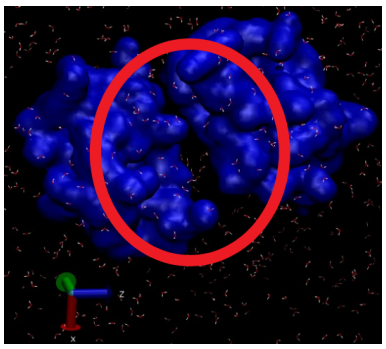

Figure 6.15: The conformational structure of Plastocyanin (PDBID:2GIM) with water contact representation Dissociation State.

As we mention before there are some water molecule which is move during the dissociation process of Plastocyanins. This number of water molecule calculate by the number which has been entering in the center of Plastocyanins which has close contact, as shown in the Figure 6.16.

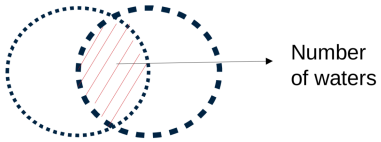

Figure 6.16: The scheme for calculation the number of water.

The exact number of water shown in table below. We can see there are the difference between each state about the number of water. In the equilibrium state which is the protein have closed contact with one another, the number of water molecule is decreasing. In other hand in transition and dissociation state the number of water molecule has been increased.

State	Number of Water
Equilibrium	16018
Transition	20163
Dissociation	21323

Table 6.3: The number of water.

This water molecule movement use an energy. The energy which is use to move water in this molecule, describe by barriers energy which is shown in Figure 6.17. It describe the reason why when entering the transition state the energy value was significantly increase. The energy has been used to move water molecule to the surface of Plastocyanins which has closed contact from one and another.

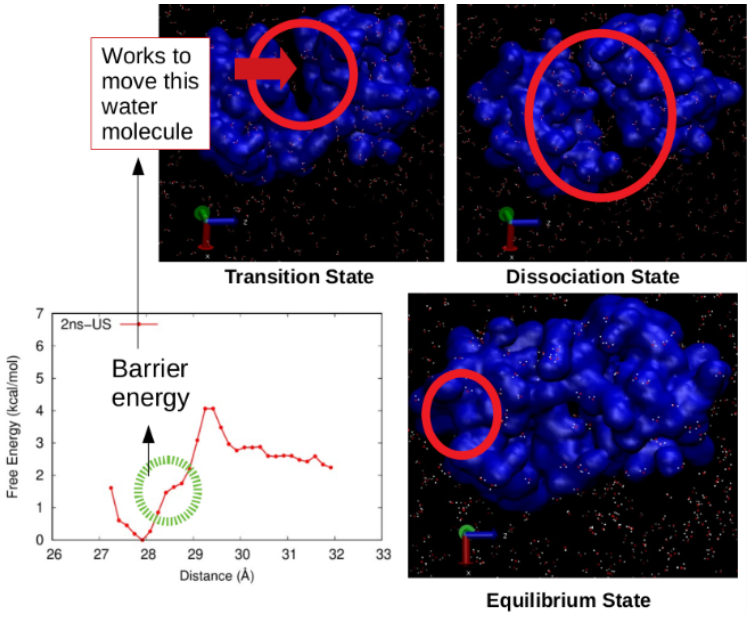

Figure 6.17: The number of water (with comparison with FEL analysis).

The number of hydrogen bonds between two Plastocyanins, show in Figure 6.18. In this figure we can see that the number of hydrogen bonds is decreasing. In Figure 6.19 and 6.20 the number of hydrogen bonds less than equilibrium state. It means the two Plastocyanins dissociating from one another.

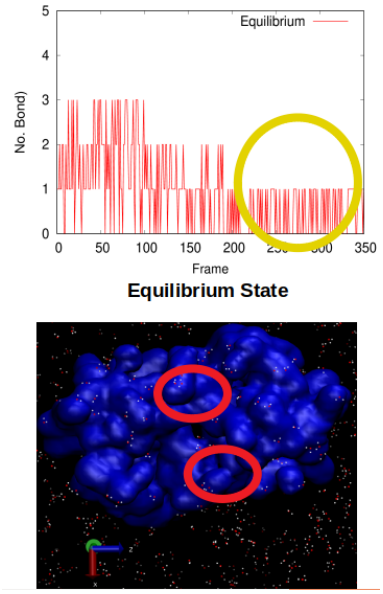

Figure 6.18: Number of hydrogen bonds between two Plastocyanin in Equilibrium state.

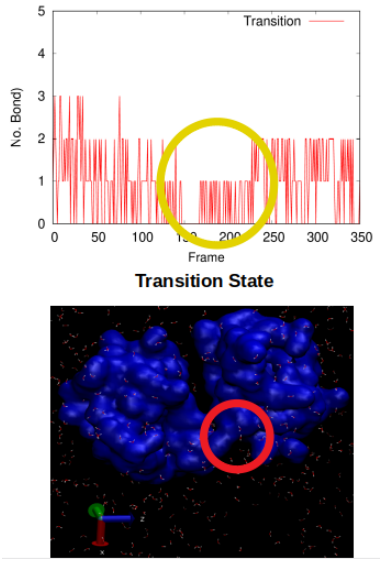

Figure 6.19: Number of hydrogen bonds between two Plastocyanin in Transition state.

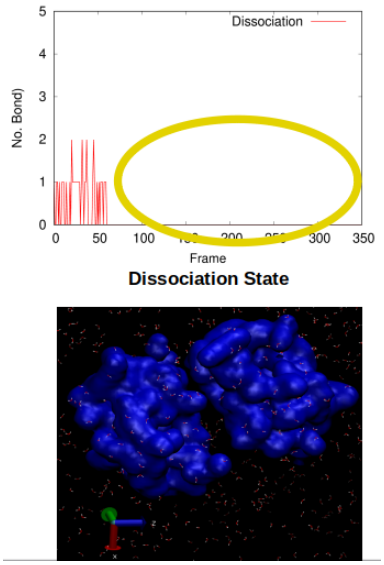

Figure 6.20: Number of hydrogen bonds between two Plastocyanin in Dissociation state.

Figure 6.21 and 6.22 show the equilibrium state for COM=28Å and COM=29Å. Figure 6.23-6.24 show the transition state for COM=30-31Å. Figure 6.25-6.26 show the dissociation state for COM=31-32Å. In each figure we can see the surface interaction between two Plastocyanins. Because of the same charge from active site, we can see the repulsive interaction between two Plastcyanins. This repulsive interaction makes Plastocyanins easily dissociate.

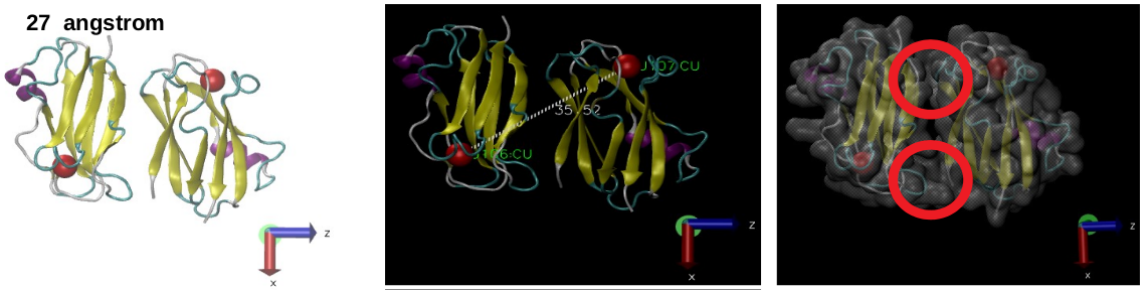

Figure 6.21: The conformational structure of Plastocyanin in Equilibrium State with COM distance=27Å.

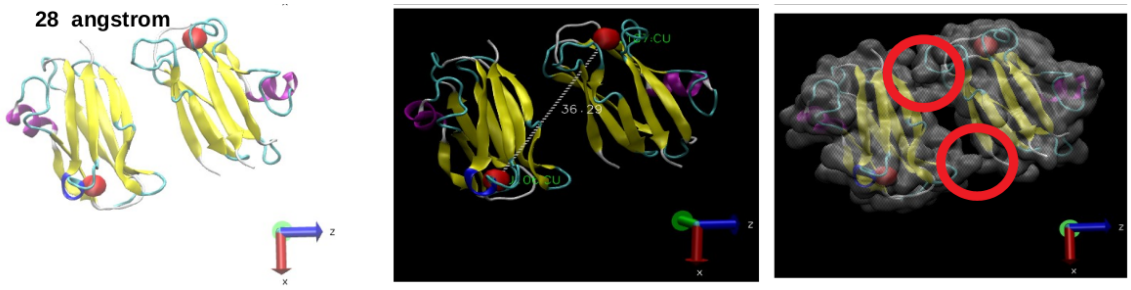

Figure 6.22: The conformational structure of Plastocyanin in Equilibrium State with COM distance=28Å.

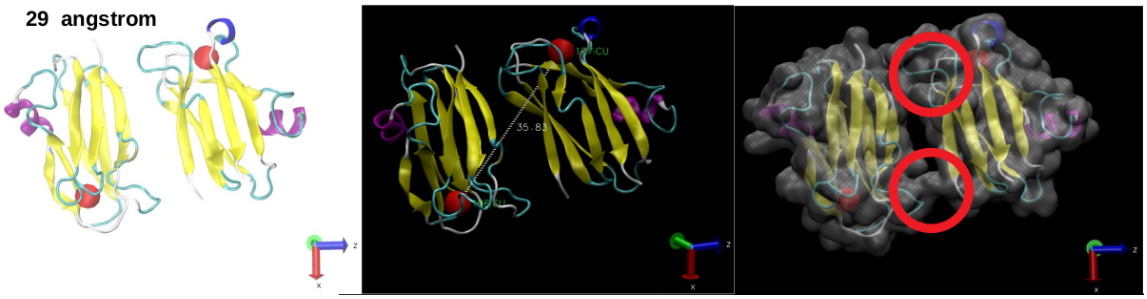

Figure 6.23: The conformational structure of Plastocyanin in Transition State with COM distance=29Å.

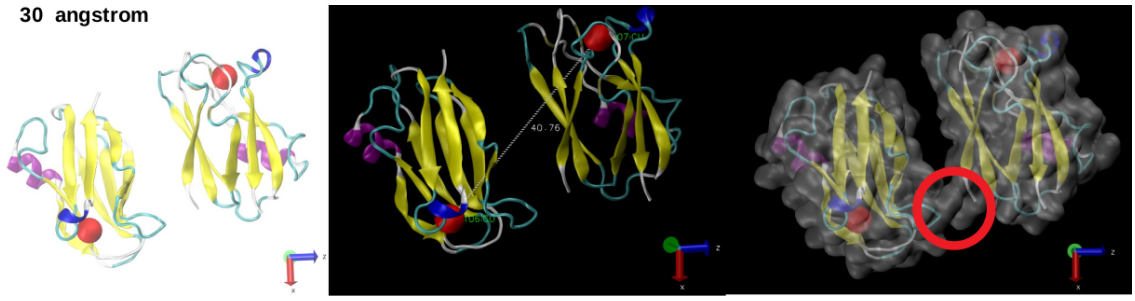

Figure 6.24: The conformational structure of Plastocyanin in Transition State with COM distance=30Å.

Figure 6.25: The conformational structure of Plastocyanin in Transition State with COM distance=31Å.

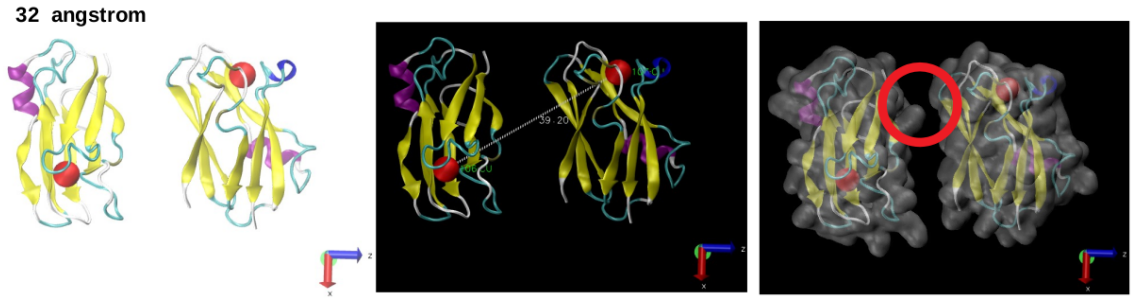

Figure 6.26: The conformational structure of Plastocyanin in Transition State with COM distance=32Å.

7 Appendix A: Theoretical Studies of Association-Dissociation Process of Plastocyanin by Coarse-Grained Simulation

7.1 Theory of Coarse Grained Model

7.2 Introduction

Cyanobacteria and unicellular green algae has plastocyanin and cyctochrome c6 (cyt) as electron carriers between b6f and photosytem I (PSI) membrane complex [15]. In this work, we present simulation for plastocyanin in A. variabilis (PDBID:2GIM). This type of plastocyanin relate to protonantion of His61 and His92. His92 spesifically, part of copper ion-binding residues. His61 influence the redox activity, although its not part of the redox centre. The important regulatory mechanism may provide this protonation histidine process [3].

We have investigated the electronic structure of active site type I copper prottein by quantum calculation [16] and free energy profile of plastocyanin to cyctochrome-f by using molecular dynamic [17], repectively.

We investigate the association-dissociation process of multi-subunit complex Plastocyanin using MARTINI coarse-grained model with PaCS-MD simulation. MARTINI coarse-grained model represent four heavy atoms, such as carbon (C), nitrogen (N), phosphor (P) become one beads. Its makes the calculation becomes less cost computational. In other hand, to generate conformation transition pathway of multi-subunit complex Plastocyanin, we use PaCS-MD simulation. This method makes the computational calculation becomes more effective using short cycle multiple independent molecular dynamics simulation to find the pathway.

We discuss about association-dissociation processes in relation to electron transfer process in the photosystem I (PSI) and the regulatory mechanism which may provide in protonation process of histidine.

7.3 Coarse-Grained Model

A coarse grained model is one kind of model which is describes few atoms in fine detail (all-atom) to a cluster. There are some kind of modelling in coarse graining. One of them is MARTINI coarse-grained method [14]. MARTINI coarse-grained method define four heavy atoms to one beads (four to one), shown in figure below.

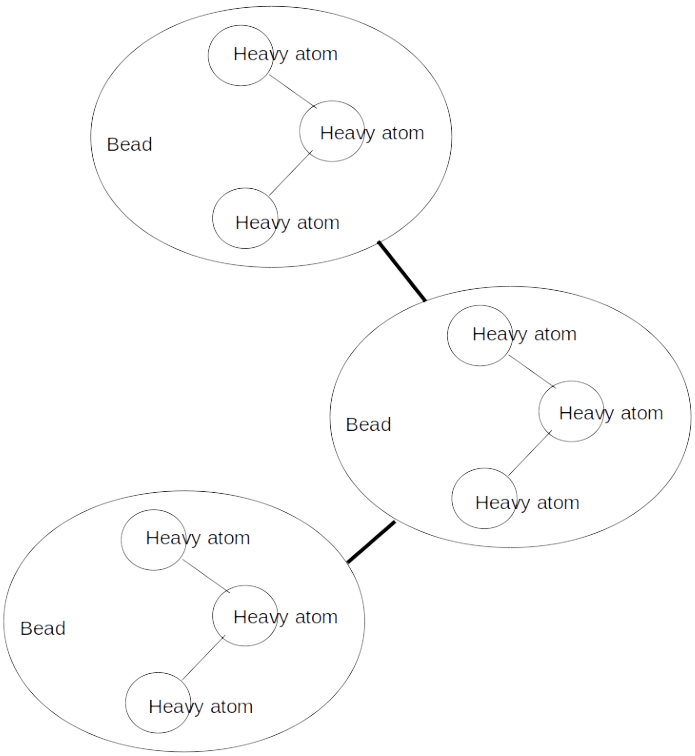

Figure 7.1: The Mapping from All-Atom (AA) Model to Coarse-Grained (CG) MARTINI Model.

This makes the accuracy for this method is less. But, the advantage for using this method is much more fast in time simulation and can describe the dynamic of complex system.

7.3.1 Interaction Sites

MARTINI coarse grained model based on four-to-one mapping. The single interaction center is described by average four heavy atom. Because the model will be keep simple, there are only four main types of interaction sites: polar (P), nonpolar (N), apolar (C) and charged (Q). The subtype number give to every particle. The reason is to make the representation more accurate for representing chemical nature of atomic structure. The difference total subtypes number has been describe from previous model, which make its increase from 9 to 18 subtypes number. The subtypes are distinguish by the capabilities of hydrogen bonding, i.e. d=donor, a=acceptor, da=both, 0=none, or by a number indicating the polarity degree (from 1 to 5, higher polarity).

7.3.2 Nonbonded Interactions

The form of the interaction potentials remains unchanged from the previous model. A shifted Lennard-Jones (LJ) 12-6 potential energy function is used to describe the nonbonded interactions

$$\vec{a} = -\frac{1}{m}\nabla E \tag{7}$$

$$U_{LJ}(r) = 4\epsilon_{ij}\left[\left(\frac{\tau_{ij}}{r}\right)^{12} - \left(\frac{\tau_{ij}}{r}\right)^{6}\right] \tag{8}$$

with τ_{ij} representing the closest distance of approach between two particles and ij the strength of their interaction. The same effective size, $\tau = 0.47$ nm, is assumed for each interaction pair, except for the two special classes of rings and antifreeze particles. In addition to the LJ interaction, charged groups (type Q) bear a full charge q_{ij} interacting via a shifted Coulombic potential energy function

$$U_{el}(r) = \frac{q_i q_j}{4\pi\epsilon_0\epsilon_r r} \tag{9}$$

with relative dielectric constant ϵ_r=15 for explicit screening. The strength of the screening has been reduced slightly (from ϵ_r= 20) with respect to the previous version of the model.

Bonded Interactions. Bonded interactions between chemically connected sites are kept unaltered with respect to the previous version of the model. Bonds are described by a weak harmonic potential V_{bond} (R)

$$V_{bond}(R) = \frac{1}{2} K_{bond} \Big(R - R_{bond} \Big)^2 \tag{10}$$

with an equilibrium distance $R_{bond} = \tau = 0.47$ nm and a force constant of $K_{bond} = 1250$ kJ mol^{-1} nm^{-1}. The LJ interaction is excluded between bonded particles. Bonded particles, on average, are somewhat closer to each other than neighboring nonbonded particles (for which the equilibrium distance is $R_{bond} = 2^{\frac{1}{6}} \tau$. To represent chain stiffness, a weak harmonic potential V_{angle} (θ) of the cosine type is used for the angles

$$V_{angle}(\theta) = \frac{1}{2} K_{angle} \Big[cos(\theta) - cos(\theta_0) \Big]^2 \tag{11}$$

LJ interactions between second nearest neighbors are not excluded. For aliphatic chains, the force constant remains at K_{angle} = 25 kJ/mol, with an equilibrium bond angle $\theta_0 = 180°$. For the angles involving the cis double bond is set to K_{angle} = 45 kJ/mol (the original value K_{angle} = 35 kJ/mol). The equilibrium angle remains at θ_0= 120°. Using the same approach for trans-unsaturated bonds, we obtain the best fit to atomistic models with an equal force constant K_{angle} = 45 kJ/mol and θ_0= 180° [14].

8 Appendix B: Theoretical Studies of Association-Dissociation Process of Plastocyanin by Coarse-Grained Simulation

8.1 Result and Disscusion

8.1.1 PaCS-MD MARTINI Coarse-Grained

The initial configuration of Plastocyanin from crystal structure with PDBID: 2GIM have been performed by MARTINI coarse-grained simulation. The equilibrium state for this complex system shown in Figure 8.1. In Figure 8.1 the red line represent the distance between center of mass of two Plastocyanin and blue line represent copper distance between two plastocyanin. The equilibrium state of the complex system which is obtained from reactive trajectories PaCS-MD All-atom molecular dynamic shown in Figure 8.1. In Figure 8.2 the red line represent the RMSD of Plastocyanin Chain A (Pc1), the blue line represent the RMSD of Plastocyanin Chain C (Pc2) and orange line represent the RMSD of Plastocyanin Chain A and Chain C (Pc1-Pc2).

The detail of parameters MARTINI coarse-grained for PaCS-MD simulation is provided in Table **??**.

Table 8.1: The parameters of MARTINI MD Simulation.

Parameters	Identities (MARTINI-MD Simulation)	Identities (MARTINI-PaCS-MD Simulation)
Simulation Program	NAMD 2.12 for linux 64-bit Intel/AMD single node	NAMD 2.12 for linux 64-bit Intel/AMD single node
Force Field	MARTINI	MARTINI
Time Step	10fs/step	10fs/step
Solvent	BP_4 model	BP_4 model
Box size	67.221 Å x 58.439 Å x 92.438 Å	67.221 Å x 58.439 Å x 92.438 Å
The number of water	7417	7417
Counter Ion	$4Na^+$, $4Cl^-$	$4Na^+$, $4Cl^-$
Temperature Control	Langevin Thermostat	Langevin Thermostat
Pressure Control	Langevin Piston	Langevin Piston
Ensemble	NPT	NPT
Cutoffs	12 Å	12 Å
Number of M runs	-	10 structure each MIMD
Simulation time	-	5 ns each MIMD

In Figure 8.1 and 8.3, there are the center of mass distance analysis for two Plastocyanins. Figure 8.1 shows the center of mass distance for two Plastocyanins by using PaCS-MD simulation with MARTINI coarse-grained model. This analysis shows with PaCS-MD simulation, the association and dissociation processes can be obtained in total simulation time around 320 ns. This total simulation time less than total simulation time in MARTINI MD simulation. In MARTINI MD simulation which is shown by Figure 8.2 the average distance of two centers of mass becomes around 30 Å for 5,6μs simulation time. This show that PaCS-MD simulation can reduce the time cost for calculating the simulation. Meanwhile in experimental data the average center of mass is 27.847 Å. The red line represent the distance between center of mass of two Plastocyanin and purple line represent copper distance between.

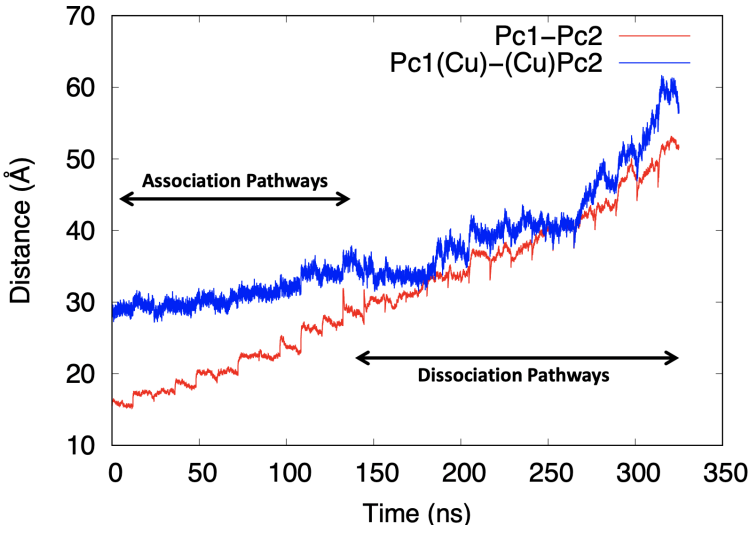

Figure 8.1: PaCS-MARTINI-MD for association-dissociation pathways, obtained by center of mass distance between two Plastocyanin corresponding to PDB file (PDB ID:2GIM). The red line represent the distance between center of mass of two Plastocyanin and blue line represent copper distance between two plastocyanin.

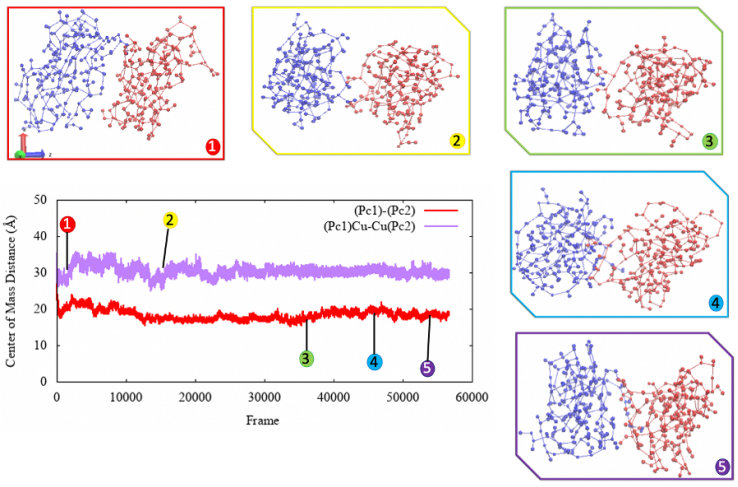

Figure 8.2: The red line represent the distance between center of mass of two Plastocyanin and purple line represent copper distance between two plastocyanin, corresponding to PDB file (PDB ID:2GIM) from CG-MARTINI-MD for describing the dissociation pathway of two complex plastocyanin. Reactive trajectories are obtained by CG-MARTINI-MD simulations (5.7μs).

Figure 8.3 and 8.4 shows the dependence of RMSD with time frame of each plastocyanins. In Figure 8.3 RMSD from PaCS-MD reactive trajectories, the red line represent the RMSD of Plastocyanin Chain A (Pc1), the blue line represent the RMSD of Plastocyanin Chain C (Pc2) and orange line represent the RMSD of Plastocyanin Chain A and Chain C (Pc1-Pc2). In Figure 8.3 the RMSD seems to fluctuate between 150-250ns simulation time. Meanwhile the RMSD from MARTINI MD simulation which is shown in Figure 8.4, seems not have significant fluctuation due to the condition of Plastocyanins that does not have any significant change during 5.6μs simulation time. In Figure 8.4 the black line represent the RMSD of Plastocyanin Chain A (Pc1), the red line represent the RMSD of Plastocyanin Chain C (Pc2) and orange line represent the RMSD of Plastocyanin Chain A and Chain C (Pc1-Pc2).

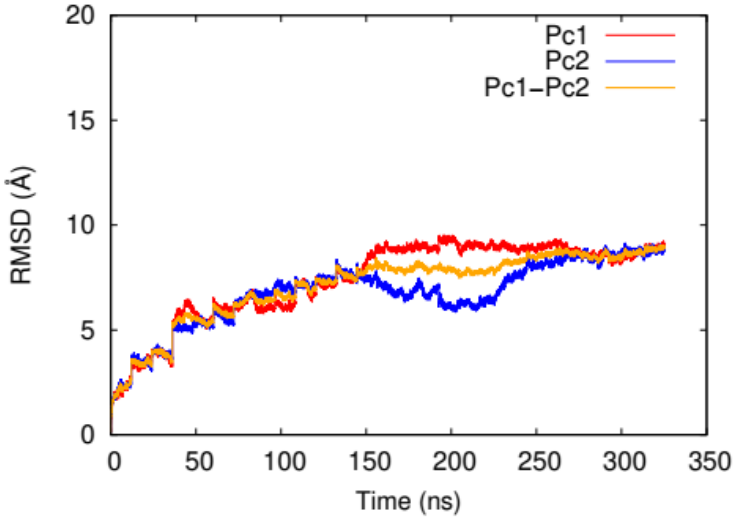

Figure 8.3: RMSD from PaCS-MARTINI-MD reactive trajectories. The red line represent the RMSD of Plastocyanin Chain A (Pc1), the blue line represent the RMSD of Plastocyanin Chain C (Pc2) and orange line represent the RMSD of Plastocyanin Chain A and Chain C (Pc1-Pc2).

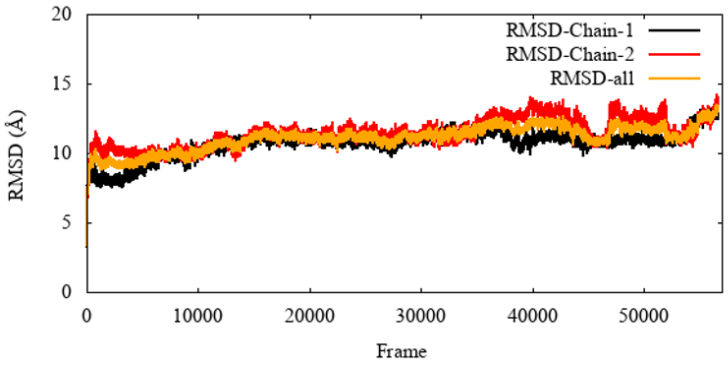

Figure 8.4: RMSD shown as time function that represent with frame, each frame steps correspond to 10 ps.

In this research, we perform PaCS-MD simulation to find the reactive trajectories of the association-dissociation process from complex Plastocyanin (PDBID:2GIM). Every ten cycle we choose the nearest COM distance (for association pathways) and the further COM distance (for dissociation pathways) of two Plastocyanin. When we compare the COM distance, its quite a difference from

original MARTINI MD, for almost 5,6μs, see Figure 8.2. The simulation remains in the dissociation process. It means regular MARTINI MD simulation can not obtain association pathways and need much more time to make complex Plastocyanin associates from one and another. From figure 2 we can see that the position of the copper ion in active site of Plastocyanin far from each other because they have repulsive interaction which much stronger for two copper ions in association pathways.

After choosing the reactive trajectories from PaCS-MD which is because the simulation time to get the association-dissociation pathways much shorter than from regular MARTINI-MD. We use that as input to calculate umbrella sampling with WHAM analysis to get free-energy landscape for association and dissociation pathways. From figure 68.5 and 8.6 we can see that when two Plastocyanin interacts with one another. The experimental value from copper-copper interaction is around 33.169$\mathring{A}$, it is quite the same with copper-copper interaction COM distance in PaCS-MD reactive trajectories for association pathways. We can see that the free energy landscape (FEL) equilibrium point is around 23$\mathring{A}$.

8.1.2 Association Pathways

In PaCS-MD simulation we calculate two pathways which describe the condition of Plastocyanins when bind with another Plastocyanins in PS I. In this part, we try to calculate the association pathways. The association pathways obtained from reactive trajectories of PaCS-MD simulation. The association pathways reach until 15$\mathring{A}$. The conformation shown in Figure 8.11 which can be seen that the Plastocyanins structure already broken.

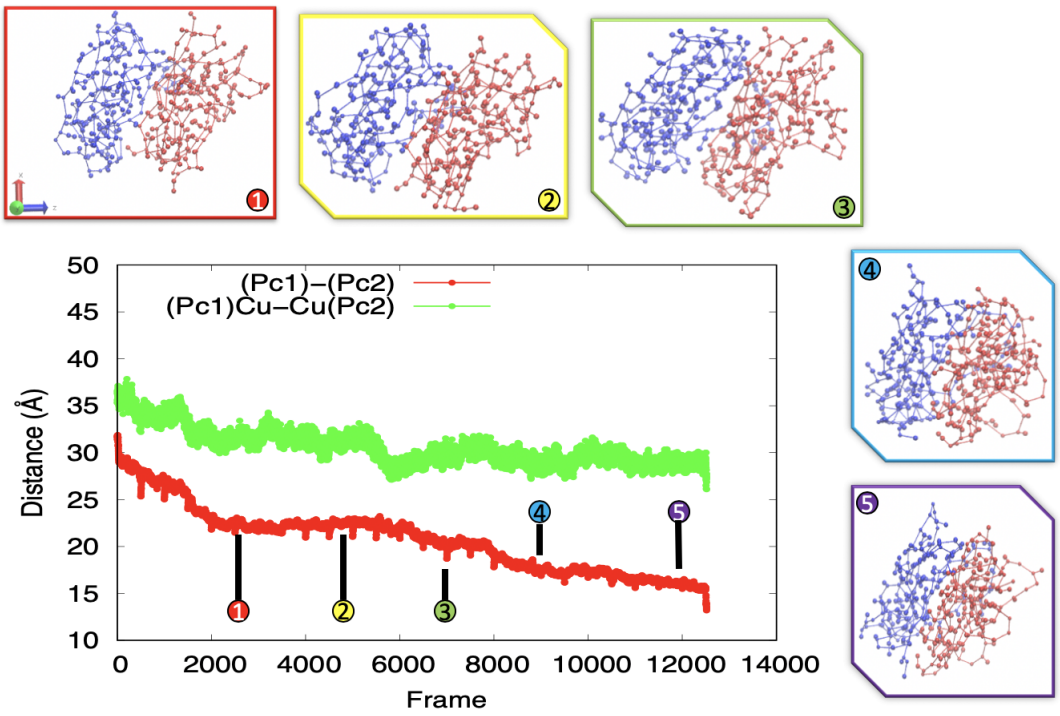

Figure 8.5: The red line represent the distance between center of mass of two Plastocyanin and green line represent copper distance between two plastocyanin, corresponding to PDB file (PDB ID:2GIM) from PaCS-CG-MARTINI-MD for describing the association pathway of two complex plastocyanin. Reactive trajectories are obtained by PaCS CG-MARTINI-MD simulations.)

8.1.3 Dissociation Pathways

The dissociation pathways obtained by PaCS-MD reactive trajectories. This pathways reach until 50$\mathring{A}$ for the distance between two Plastocyanins. This condition means the dissociation pathways can happen because the repulsive interaction between two Plastocyanins.

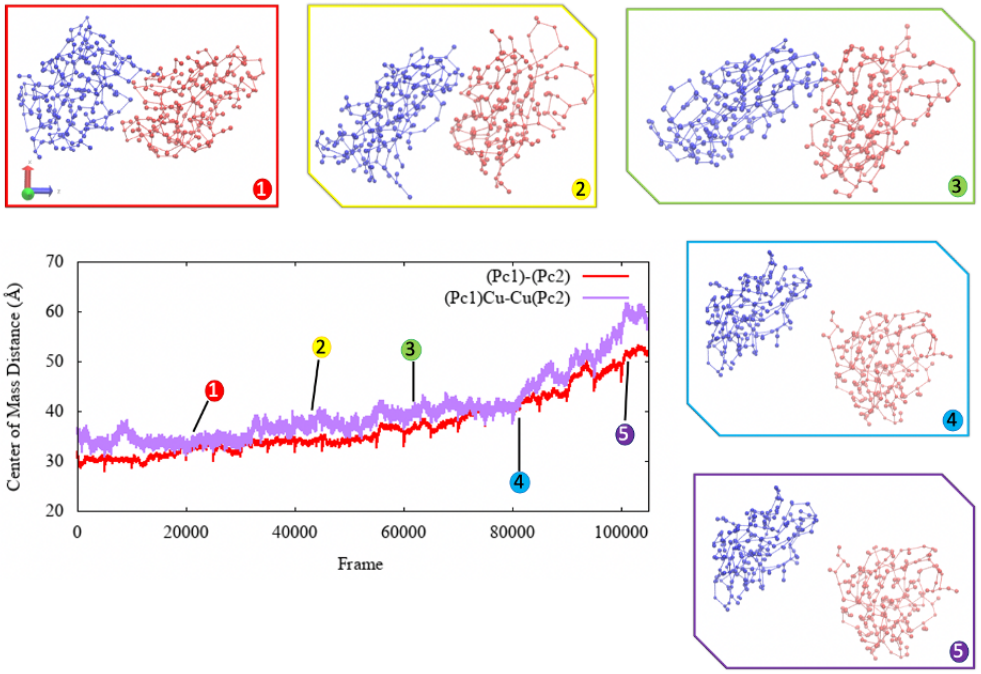

Figure 8.6: The red line represent the distance between center of mass of two Plastocyanin and purple line represent copper distance between two plastocyanin, corresponding to PDB file (PDB ID:2GIM) from PaCS-CG-MARTINI-MD for describing the dissociation pathway of two complex plastocyanin. Reactive trajectories are obtained by PaCS CG-MARTINI-MD simulations.)

8.2 Free Energy Landscape (FEL) Analysis

The free energy landscape shown in Figure 8.8 with probability distribution in Figure 8.7. The probability distribution shows the distribution of total sampling each COM distance. In Figure 8.8 we can see that the free energy dissociation bigger than the all-atom simulation value. We assume because the representation of the model reduce the degree of freedom. It can be shown that the equilibrium point around 26$\mathring{A}$. In Figure 8.8 we can see in dissociation process the free energy

become reduce which is not suitable with the disociation process condition. It can be seen in the probability distribution in Figure 8.7. In Figure 8.7 we can see that the sampling is still lacking. So we try to add the sampling for dissociation pathways. There is significant change in FEL shown in figure 8.10. The free energy for dissociation process quite more constant after that.

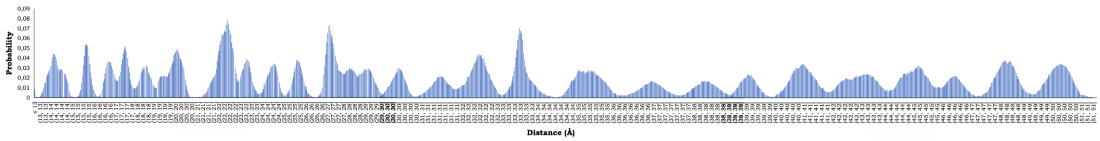

Figure 8.7: Probability distribution in each COM distance for force constant=5 kcal/mol.

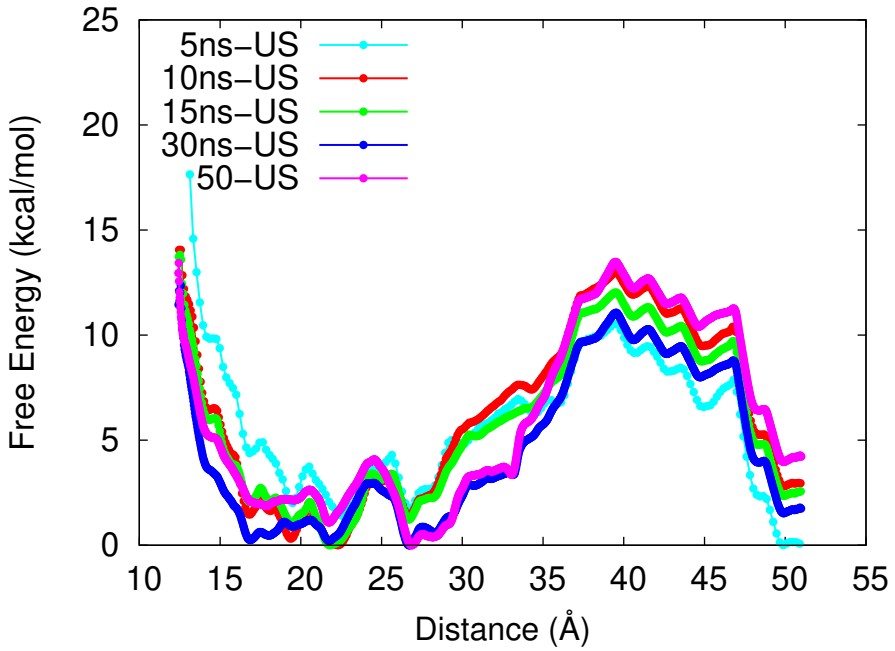

Figure 8.8: Free energy landscape from Umbrella sampling analysis with WHAM (force constant=5 kcal/mol). Equilibration point=26.851$\mathring{A}$.

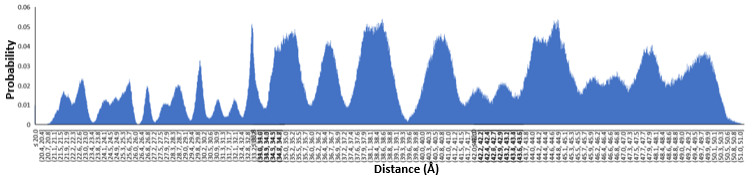

Figure 8.9: Probability distribution in each COM distance for force constant=5 kcal/mol.

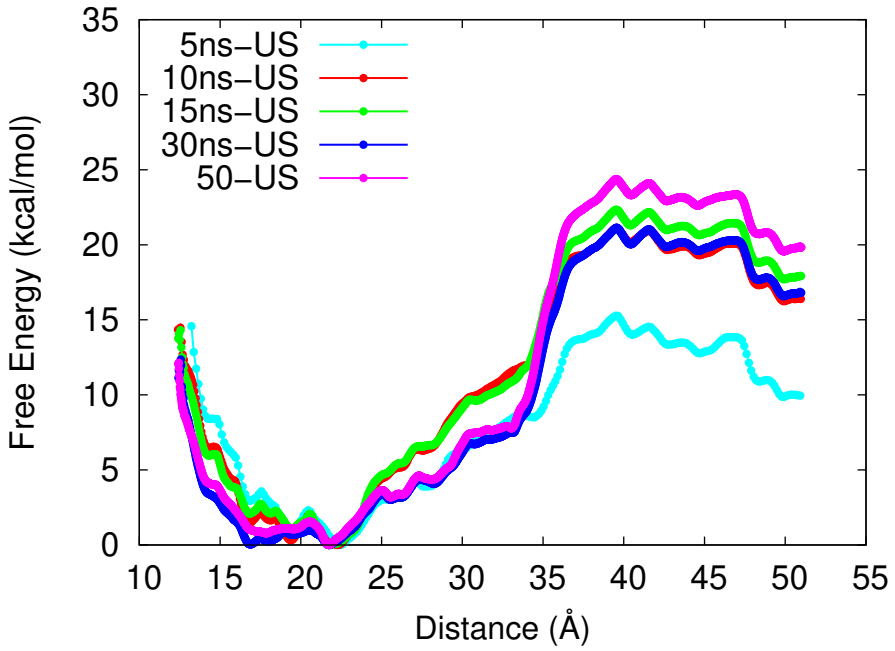

Figure 8.10: Free energy landscape from Umbrella sampling analysis with WHAM (force constant=5 kcal/mol).

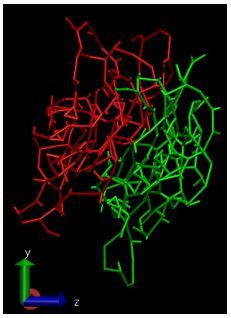

Figure 8.11: The conformational structure of Plastocyanin (PDBID:2GIM), the center of mass distance between two Plastocyanins = 15$\mathring{A}$.

The conformational structure for some center of mass distance, shown in figure belows.

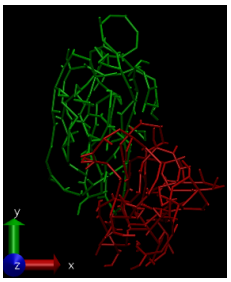

Figure 8.12: The conformational structure of Plastocyanin (PDBID:2GIM), the center of mass distance between two Plastocyanins = 22$\mathring{A}$.

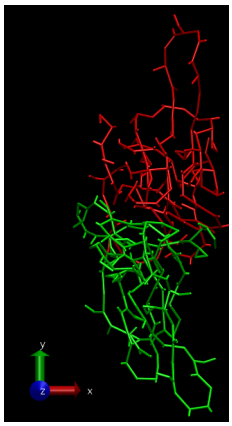

Figure 8.13: The conformational structure of Plastocyanin (PDBID:2GIM), the center of mass distance between two Plastocyanins = 27$\mathring{A}$.

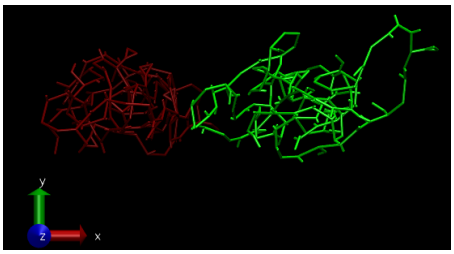

Figure 8.14: The conformational structure of Plastocyanin (PDBID:2GIM), the center of mass distance between two Plastocyanins = 29$\mathring{A}$.

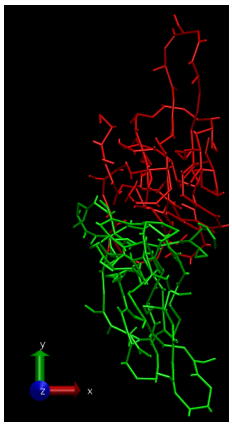

Figure 8.15: The conformational structure of Plastocyanin (PDBID:2GIM), the center of mass distance between two Plastocyanins = 33$\mathring{A}$.

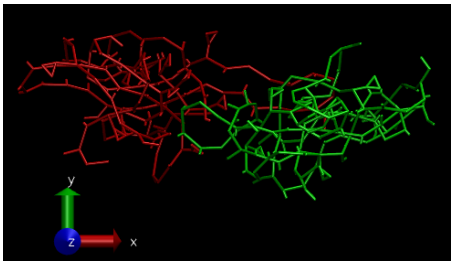

Figure 8.16: The conformational structure of Plastocyanin (PDBID:2GIM), the center of mass distance between two Plastocyanins = 35$\mathring{A}$.

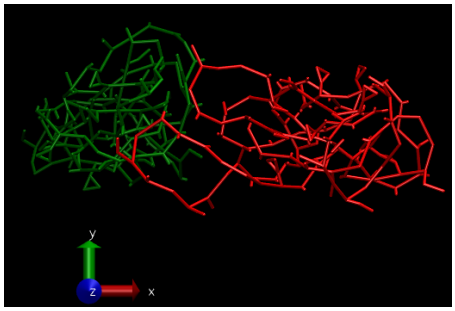

Figure 8.17: The conformational structure of Plastocyanin (PDBID:2GIM), the center of mass distance between two Plastocyanins = 40$\mathring{A}$.

8.3 Summary

8.3.1 PaCS-MD All-Atom

We have presented a procedure of calculation of free energy landscape of two proteins by using parallel cascade molecular dynamics (PaCS-MD) and multiple independent umbrella sampling (MIUS). The free energy landscape of two plastocyanins for association/dissociation process has been investigated by using the present method. We have found that binding free energy is around 3 kcal/mol and that the barrier energy at around the middle range between the equilibrium point and the dissociation state becomes about 1 kcal/mol from the association process. The present results suggest that the energy barrier may arise from hydrogen bonds between two plastocyanins. We have also found that the effective interaction between two plastocyanins already vanishes at the distance of 2 $\mathring{A}$ from equilibrium state. The equilibrium point of the complex around 27.9 $\mathring{A}$ is a good agreement with the experimental result 27.8 $\mathring{A}$.

8.3.2 PaCS-MD MARTINI Coarse-Grained

We have presented a procedure of calculation of free energy landscape of two proteins by using parallel cascade molecular dynamics (PaCS-MD) and multiple independent umbrella sampling (MIUS). The free energy landscape of two plastocyanins for association/dissociation process has been investigated by using the present method. We have found that binding free energy is around 3 kcal/mol and that the barrier energy at around the middle range between the equilibrium point and the dissociation state becomes about 1 kcal/mol from the association process. The present results suggest that the energy barrier may arise from hydrogen bonds between two plastocyanins. We have also found that the effective interaction between two plastocyanins already vanishes at the distance of 2 $\mathring{A}$ from equilibrium state. The equilibrium point of the complex around 27.9 $\mathring{A}$ is a good agreement with the experimental result 27.8 $\mathring{A}$.

References

[1] Jez J 2021 Photosynthesis — The Photosystem I Complex of Oxygenic Photosynthesis 191-206.

[2] Lennarz W J and Lane M D 2013 Encyclopedia of Biological Chemistry (Second Edition) *Academic Press* 530-532.

[3] Schmidt L, Christensen, H E M and Harris P 2006 *Acta Crystallographica Section D* **62** 1022-1029.

[4] Sigfridsson K 1998 Plastocyanin, an electron-transfer protein *Photosynthesis Research* **57** 1–28.

[5] `https://www.dovepress.com/cr_data/article_fulltext/s70000/70333/img/fig3.jpg`

[6] Hospital A, Goñi JR, Orozco M, Gelpi J 2015 Molecular dynamics simulations: advances and applications *Adv Appl Bioinform Chem* **8** 37-47. https://doi.org/10.2147/AABC.S70333

[7] Brooks B R, Brooks III C L, MacKerell, Jr. A D, Nilsson L, Petrella R J, Roux B, Won Y, Archontis G, Bartels C, Boresch S, Caflisch A, Caves L, Cui Q, Dinner A R, Feig M, Fischer S, Gao J, Hodoscek M, Im W, Kuczera K, Lazaridis T, Ma J, Ovchinnikov V, Paci E, Pastor R W, Post C B, Pu J Z, Schaefer M, Tidor B, Venable R M, Woodcock H L, Wu X, Yang W, York D M, and Karplus M 2009 *J. Comput. Chem.* **30** 1545-1614.

[8] Harada R and Kitao A 2013 *The Journal of Chemical Physics* **139**(3) 0351103.

[9] MacKerell Jr., A.D., Feig, M., and Brooks, III, C.L. 2004 *Journal of Computational Chemistry* **25** 1400-1415, 2004.

[10] https://www.ks.uiuc.edu/Research/vmd/current/ug/node194.html

[11] Phillips J C, Hardy D J, Maia J D C, Stone J E, Ribeiro J V, Bernardi R C, Buch R, Fiorin G, Henin J, Jiang W, McGreevy R, Melo M C R, Radak B K, Skeel R D, Singharoy A, Wang Y, Roux B, Aksimentiev A, Luthey-Schulten Z, Kale L V, Schulten K, Chipot C, and Tajkhorshid E 2020 *Journal of Chemical Physics* **153** 044130.

[12] Lee J, Cheng X, Swails J M, Yeom M S, Eastman P K, Lemkul J A, Wei S, Buckner J, Jeong J C, Qi Y, Jo S, Pande V S, Case D A, Brooks III C L, MacKerell Jr A D, Klauda J B and Im W 2016 *J. Comput. Chem.* **12** 405-413.

[13] Jorgensen W L, Chandrasekhar J, Madura J D, Impey R W and Klein M L 1983 *The Journal of Chemical Physics.* **79**(2) 926-935.

[14] Marrink S 2007 The martini force field: Coarse grained model for biomolecular simulations *Journal of Physical Chemistry B* **111** 7812-7824.

[15] Bernal-Bayard P, Pallara C, Carmen C M, Molina-Heredia FP, Fernandez-Recio J, Hervas M, Navarro J A 2015 Interaction of photosystem I from Phaeodactylum tricornutum with plastocyanins as compared with its native cytochrome c6: Reunion with a lost donor *Biochim Biophys Acta.* **1847**(12) 1549-59.

[16] Kurniawan I, Kawaguchi K, Sugimori K, Sakurai T and Nagao H 2019 *Sci. Rep. Kanazawa Univ.* **63** 1-13. 012026.

[17] Kurniawan I, Matsui, T, Nakagawa S, Kawaguchi K and Nagao H 2018 *IOP Conf. Series: Journal of Physics: Conf. Series* **012026**(1136) 1-12.

[18] Davis D J, Krogmann D W and Pietro A S 1980 *Plant Physiology* **65**(4) 697-702.

[19] Hope A B 2000 *Biochimica et Biophysica Acta (BBA) - Bioenergetics* **1456**(1) 5-26.

[20] Redinbo M R, Yeates T O and Merchant S 1994 *J Bioenerg Biomembr* **26** 49-66.

[21] Cattani G, Vogeley L, and Crowley P B 2015 *Nature chemistry* **7**(10) 823-828.

Appendix

Figure 8.18: Conformation of 2GIM from 13Å, fc=1.5 kcal/mol

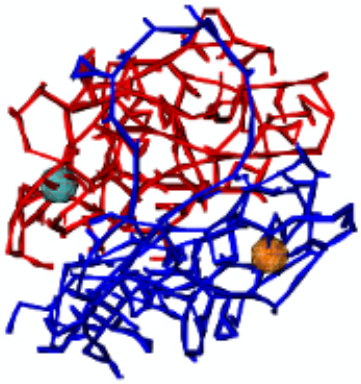

2GIM conformation in 13Å COM distance

chain A side view

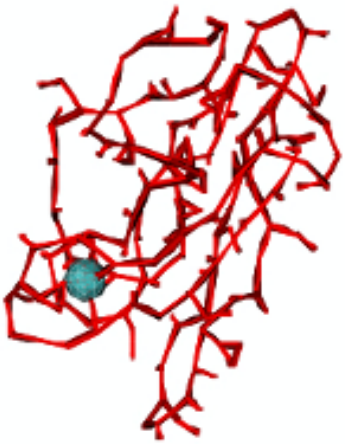

chain C side view

Figure 8.19: Conformation of 2GIM from 14Å, fc=1.5 kcal/mol

2GIM conformation in 14Å COM distance

chain A side view

chain C side view

Figure 8.20: Conformation of 2GIM from 15Å, fc=1.5 kcal/mol

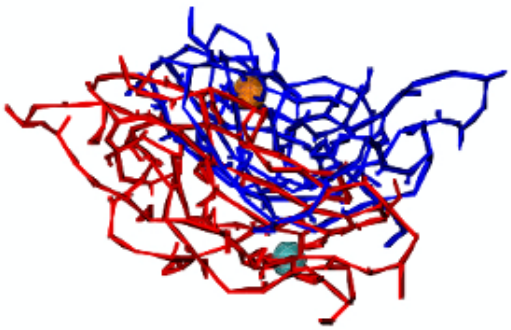

2GIM conformation in 15Å COM distance

chain A side view

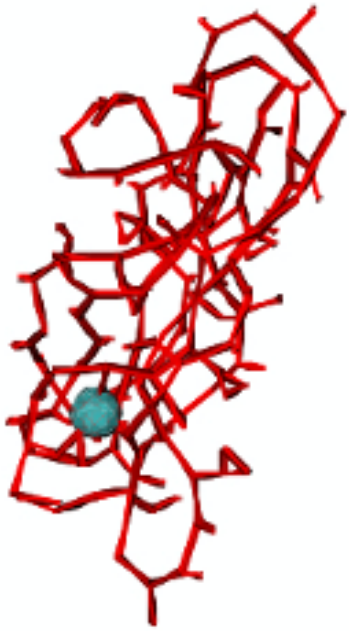

chain C side view

Figure 8.21: Conformation of 2GIM from 16Å, fc=1.5 kcal/mol

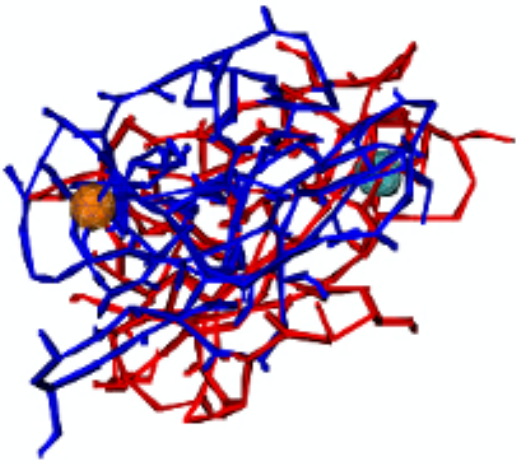

2GIM conformation in 16Å COM distance

chain A side view

chain C side view

Figure 8.22: Conformation of 2GIM from 17Å

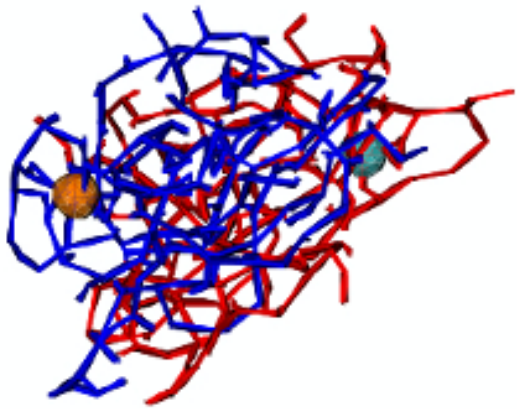

2GIM conformation in 17Å COM distance, fc=1.5 kcal/mol

chain A side view

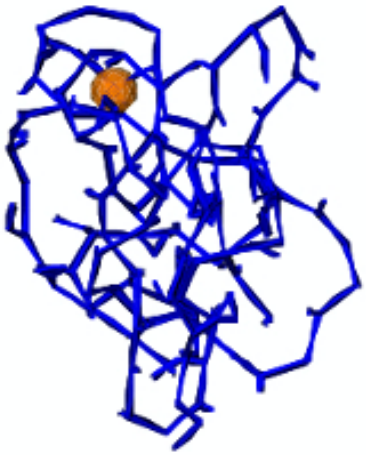

chain C side view

Figure 8.23: Conformation of 2GIM from 18Å

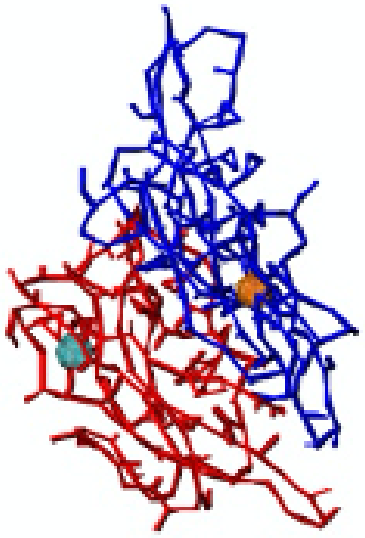

2GIM conformation in 18Å COM distance, fc=1.5 kcal/mol

chain A side view

chain C side view

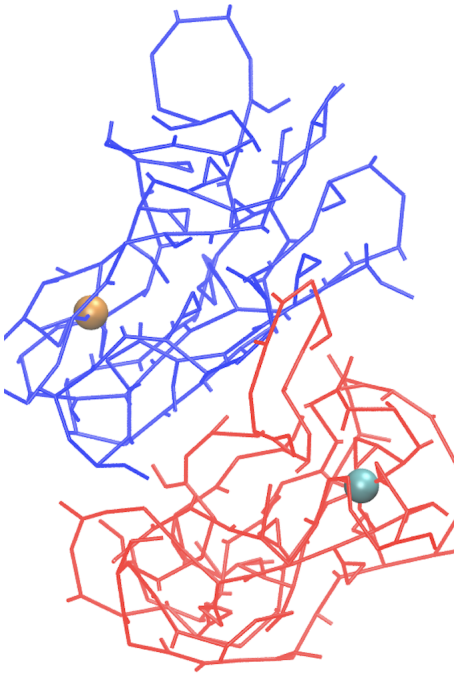

Figure 8.24: 2GIM conformation in 25Å COM distance, fc=1 kcal/mol

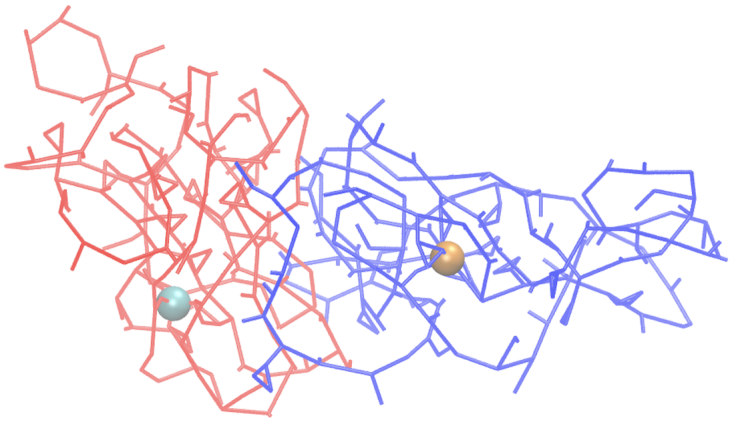

Figure 8.25: 2GIM conformation in 26Å COM distance, fc=1 kcal/mol

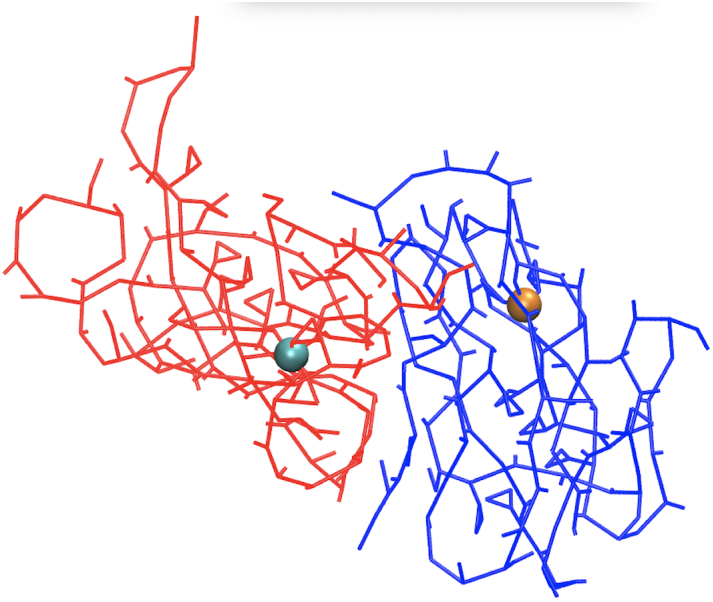

Figure 8.26: 2GIM conformation in 27Å COM distance, fc=1 kcal/mol

Figure 8.27: 2GIM conformation in 28Å COM distance, fc=1 kcal/mol

Figure 8.28: Conformation of 2GIM from 13Å, fc=0.1 kcal/mol

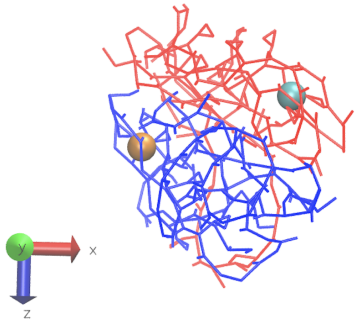

2GIM conformation in 13Å COM distance

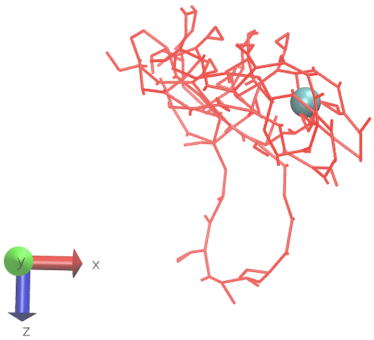

chain A side view

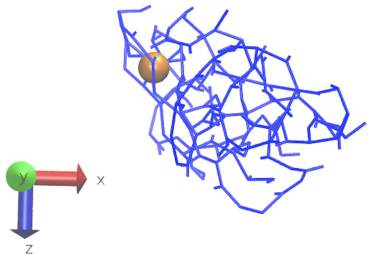

chain C side view

Figure 8.29: Conformation of 2GIM from 14Å, fc=0.1 kcal/mol

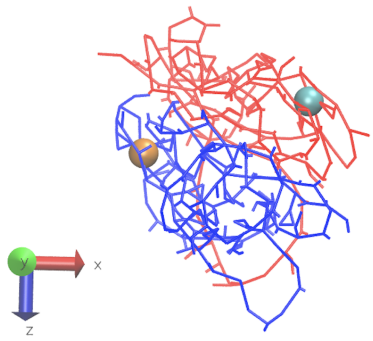

2GIM conformation in 14Å COM distance

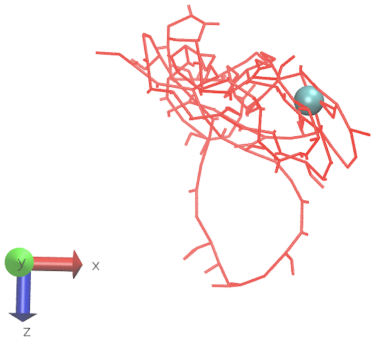

chain A side view

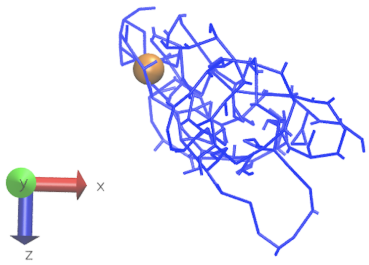

chain C side view

Figure 8.30: Conformation of 2GIM from 15Å, fc=0.1 kcal/mol

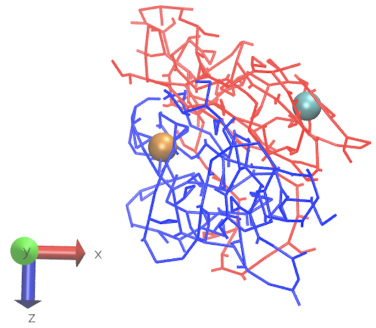

2GIM conformation in 15Å COM distance

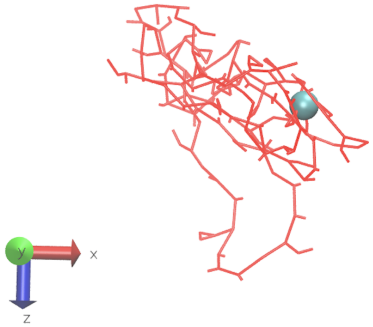

chain A side view

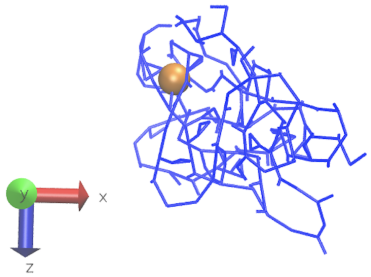

chain C side view

Figure 8.31: Conformation of 2GIM from 16Å, fc=0.1 kcal/mol

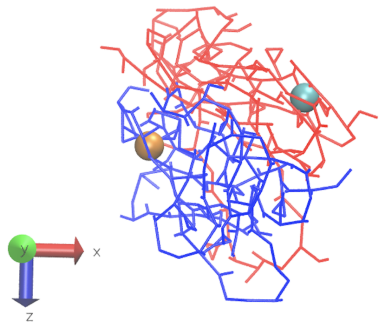

2GIM conformation in 16Å COM distance

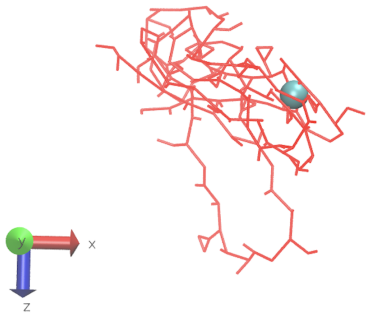

chain A side view

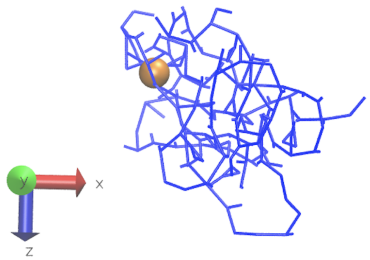

chain C side view

Figure 8.32: Conformation of 2GIM from 17Å, fc=0.1 kcal/mol

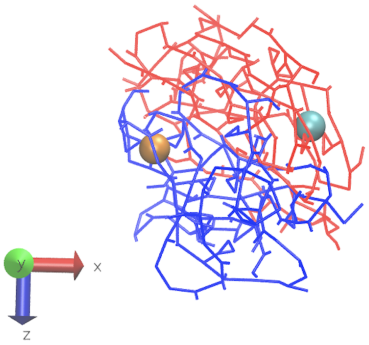

2GIM conformation in 17Å COM distance

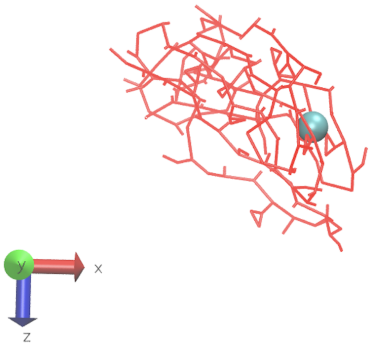

chain A side view

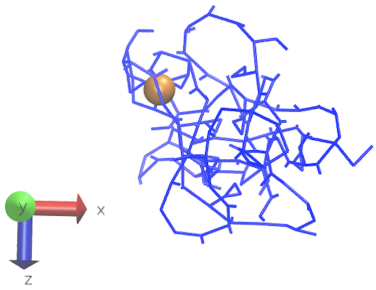

chain C side view

Figure 8.33: Conformation of 2GIM from 18Å, fc=0.1 kcal/mol

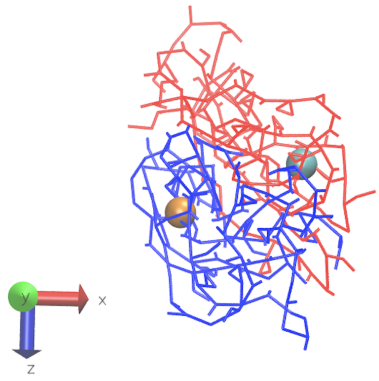

2GIM conformation in 18Å COM distance

chain A side view

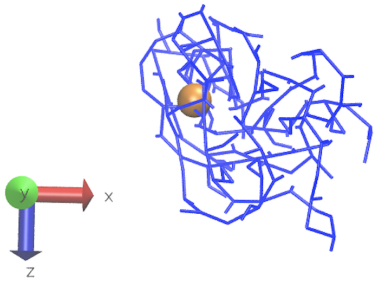

chain C side view

Figure 8.34: Conformation of 2GIM from 19Å, fc=0.1 kcal/mol

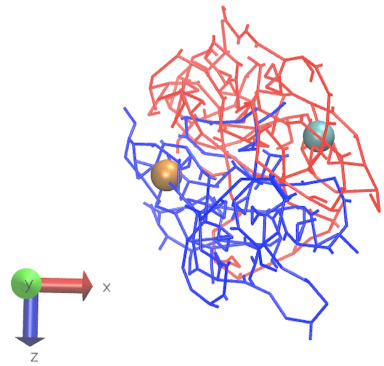

2GIM conformation in 19Å COM distance

chain A side view

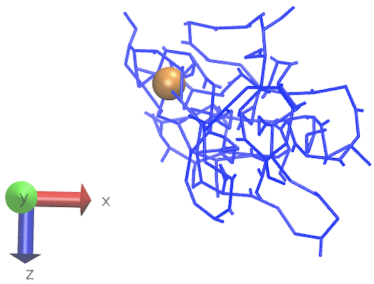

chain C side view

Figure 8.35: Conformation of 2GIM from 20Å, fc=0.1 kcal/mol

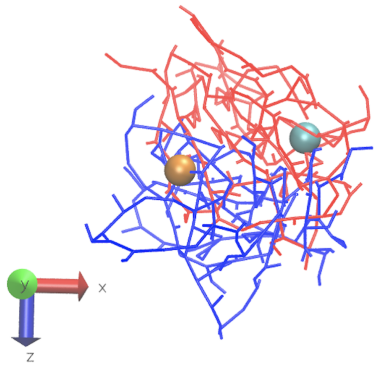

2GIM conformation in 20Å COM distance

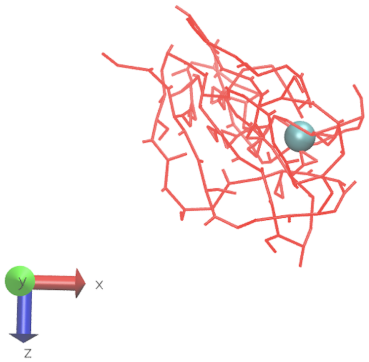

chain A side view

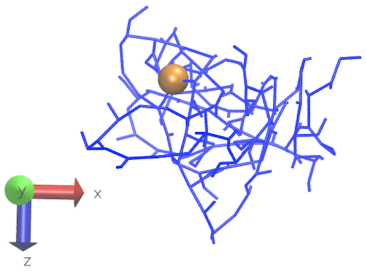

chain C side view

Figure 8.36: Conformation of 2GIM from 13Å, fc=0.001 kcal/mol

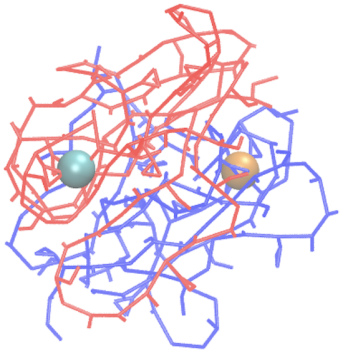

2GIM conformation in 13Å COM distance

chain A side view

chain C side view

Figure 8.37: Conformation of 2GIM from 14Å, fc=0.001 kcal/mol

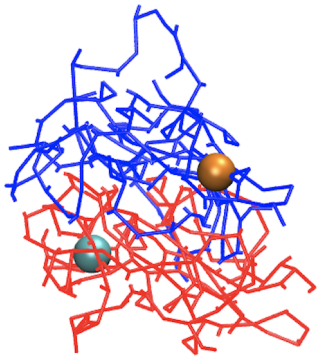

2GIM conformation in 14Å COM distance

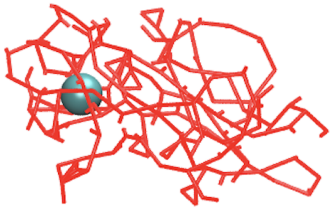

chain A side view

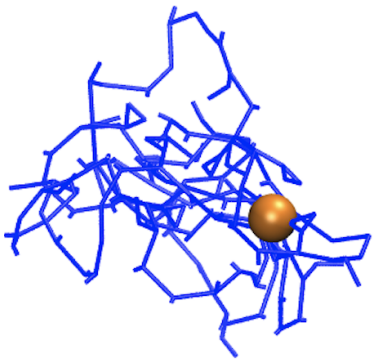

chain C side view

Figure 8.38: Conformation of 2GIM from 15Å, fc=0.001 kcal/mol

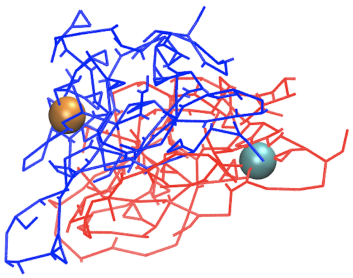

2GIM conformation in 15Å COM distance

chain A side view

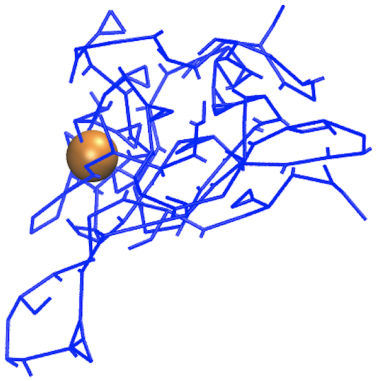

chain C side view

Figure 8.39: Conformation of 2GIM from 16Å, fc=0.001 kcal/mol

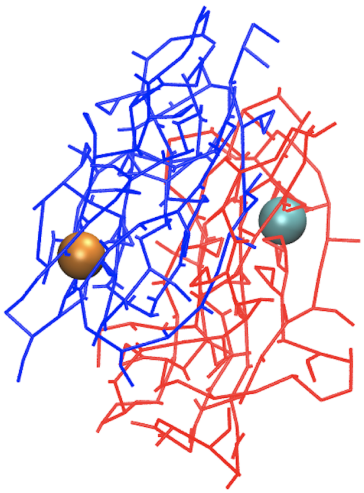

2GIM conformation in 16Å COM distance

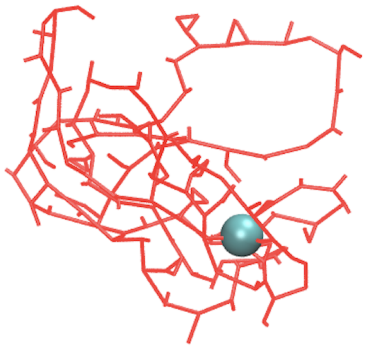

chain A side view

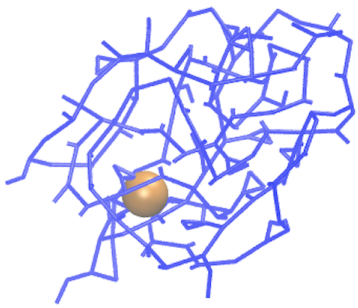

chain C side view

Figure 8.40: Conformation of 2GIM from 17Å, fc=0.001 kcal/mol

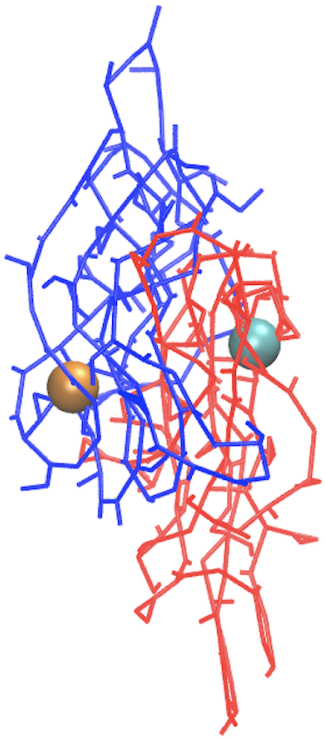

.

2GIM conformation in 17Å COM distance

chain A side view

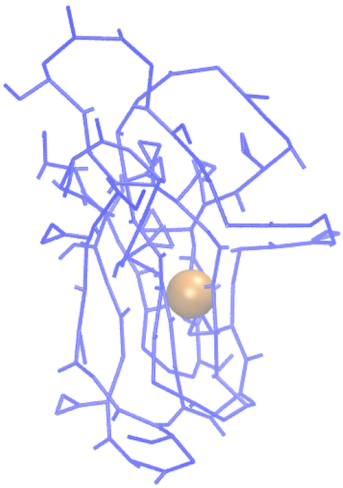

chain C side view